REMARKS/ARGUMENTS

The Examiner's attention to the present application is noted with appreciation.

Objection to the Specification. The specification has been amended and arranged as suggested at pages 2 and 3 of the Office Action. It is noted that the text under "BRIEF DESCRIPTION OF THE DRAWINGS" is directly derived from the specification, and no new matter is added.

The title is amended, to "Bleomycin and Virus-Inhibiting Combination Pharmaceutical Composition and Methods." It is submitted that this title is descriptive.

35 U.S.C. § 112, Second Paragraph, Rejection of claims 1 - 6. Claims 1 - 6 were rejected as being indefinite for failing to particularly point out and distinctly claim the subject matter. The claims have been extensively amended, and it is submitted that this ground of rejection has been overcome.

35 U.S.C. § 112, First Paragraph, Rejection of claims 1 - 6. Claims 1 - 6 are rejected as containing subject matter which was not described in the specification in such a way as to enable one skilled in the art to which it pertains, or with which it is most nearly connected, to make and/or use the invention. This is an enablement rejection.

It is initially noted that claims 1 - 7 as amended are drawn to a "pharmaceutical product." Additionally, the scope of claim 1 has been narrowed to bleomycin in combination with a virus-inhibiting agent. Such a combination is specifically shown in the Examples (specification at 10, lines 21 – 24).

MPEP § 2164.08 makes clear that "[a]ll question of enablement are evaluated against the claimed subject matter. The focus of the examination inquiry is whether everything within the scope of the claim is enabled." The scope of claims 1 - 7 are a "pharmaceutical product", specifically one which comprises "bleomycin" and a "virus-inhibiting compound." The specification teaches such a specific pharmaceutical product (see, e.g., specification at 10, lines 21 – 24) which was actually made. Additionally, there is nothing in the combining of two ingredients to make a novel pharmaceutical product which is uncertain or would require undue experimentation. While the question of utility under section 101 is separate from

BEST AVAILABLE COPY

enablement under section 112, there is no doubt that in vitro results are sufficient to establish utility. See, e.g., MPEP § 2107 (c).

With respect to claims 8 - 13, it is noted that the claims are drawn narrowly to bleomycin and a virus-inhibiting compound. Bleomycin is well known as a chemotherapeutic agent, and is well characterized. The two specific virus-inhibiting compounds disclosed, ritonavir and dideoxinosine, are both known pharmaceutical compounds, used in the treatment of HIV infection. Thus the concerns raised in the office action, e.g., "exposure to the target site", "biological stability", "half-life," "clearance," potential "proteolytic degradation or immunological activation", "inability to penetrate tissues or cells", and so on are not relevant. Bleomycin has long been used in treatment of various cancers. Virus-inhibiting compounds have long been used in treatment of HIV infection and other viral diseases. Given the narrow nature of the claims, the specification is enabled. There would be no undue experimentation. Patients with HIV infection are commonly given virus-inhibiting compounds; practice of the invention simply involves administration of a second and very specific drug, bleomycin. It is difficult to hypothesize a simpler and more straight-forward factual scenario for a novel method of treating a disease where, at the time of the filing of the patent application, there was not yet human clinical data.

Claims 14 to 27 are similarly narrowly drawn to an iron chelator that is hydroxypyridinon, such as deferiprone, in combination with a virus-inhibiting compound. Hydroxypyridinons, such as deferiprone, are similarly known agents and are well characterized and studied.

35 U.S.C. § 102(b) Rejection of claims 1 - 2. Claims 1 and 2 are rejected as being anticipated by Tabor et al. This rejection is respectfully traversed. Claim 2 has been canceled, and claim 1 amended such that it is limited to bleomycin, and not an iron chelator generally. Tabor et al. teach, as the Office Action notes, hydroxamate derivatives such as deferoxamine. The claim as amended is drawn to bleomycin, which is neither suggested nor taught by Tabor et al. Similarly, claims 14 - 27 are directed to an iron chelator that is hydroxypyridinon, such as deferiprone. A hydroxamate derivative is chemical different and distinct from a hydroxypyridinon.

35 U.S.C. § 102(b) Rejection of claims 1, 2, 5 and 6. Claims 1, 2, 5 and 6 are rejected as being anticipated by Malley et al. This rejection is respectfully traversed. Claim 1 has been amended, such that it is limited to bleomycin, and not iron chelators generally. As with Tabor et al., Malley et al. specifically teach use of hydroxamate compounds, and neither teaches nor anticipates use of bleomycin. Similarly, claims 14 - 27 are directed to an iron chelator that is hydroxypyridinon, such as deferiprone. A hydroxamate derivative is chemical different and distinct from a hydroxypyridinon.

35 U.S.C. § 103 Rejection of claims 1 - 4. Claims 1 - 6 are rejected as obvious over Malley et al. in view of Sham et al. This rejection is respectfully traversed. Sham et al. teach use of retonavir. Malley et al. teach use of hydroxamates. Claim 1, as well as new claim 8, is drawn to a product and method, respectively, using bleomycin. New independent claims 14 and 20 are drawn to a product and method, respectively, using a hydroxypyridinon, such as deferiprone.

Thus the invention as now claimed is not obvious over prior art teaching hydroxamates.

The prior art with respect to hydroxamates does not make obvious use of bleomycin. Hydroxamates chelate iron and thereafter protect against hydrogen peroxide-induced activation of HIV-1, as taught by Sappey et al. (*AIDS Research Human Retroviruses*) (copy enclosed, see abstract and page 1058, second column). In contrast, it is known that bleomycin chelated iron increases the formation of oxygen radicals, including superoxide, H_2O_2. See, e.g., Day et al. (*Am J Physiol Lung Cell Mol Physiol*) (copy enclosed, see page L1342, second column, first full paragraph.

The difference in pharmacological and physiological action between hydroxamates and bleomycin may be seen by examining Fig. 4 of the application and the text at page 9, line 25 through page 10, line 5. Comparing deferoxamine (panel A) with bleomycin (panel C), it is seen that while both decreased viral replication (p24 antigen panel), deferoxamine caused significant lymphocyte cytotoxicity (viable cell count panel) while bleomycin did not (viable cell count panel). Compare also Fig. 1 (deferoxamine cell count and proliferation) with Fig. 3 (bleomycin cell count and proliferation). As stated in the specification at 2, lines 23 – 25, bleomycin inhibited viral replication without affecting lymphocyte proliferation. Thus, the

specification provides evidence that inhibition of HIV-1 proliferation by bleomycin proceeds via a different pathway from that of hydroxamates such as deferoxamine.

Finally, the combination index (see Fig. 6) for bleomycin and ritonavir shows a synergistic effect between the two active ingredients.

Similarly, there is no teaching or suggestion in the prior art of record that a hydroxypyridinon could be substituted for a hydroxamate in the treatment of viral diseases such as HIV infection.

Conclusion. In view of the above amendments and remarks, it is respectfully submitted that all grounds of rejection and objection have been avoided and/or traversed. It is believed that the case is now in condition for allowance and same is respectfully requested.

If any issues remain, or if the Examiner believes that prosecution of this application might be expedited by discussion of the issues, the Examiner is cordially invited to telephone the undersigned attorney for Applicant at the telephone number listed below.

A check for additional claims is enclosed. Also being filed herewith is a Petition for Extension of Time to August 11, 2004, with the appropriate fee. Authorization is given to charge payment of any additional fees required, or credit any overpayment, to Deposit Acct. 13-4213.

Respectfully submitted,

By: 

Stephen A. Slusher, Reg. No. 43,924
Direct line: (505) 998-6130

PEACOCK, MYERS & ADAMS, P.C.
Attorneys for Applicant(s)
P.O. Box 26927
Albuquerque, New Mexico 87125-6927

Telephone: (505) 998-1500
Facsimile: (505) 243-2542

Customer No. 005179

[G:\AMDS\Los&Stig\Van Asbeck HIV 579 OAR.doc]

12. Juli 2004 14:49 Lee & Stigter Nr. 0319 P. 4

1012825

AIDS RESEARCH AND HUMAN RETROVIRUSES
Volume 11, Number 9, 1995
Mary Ann Liebert, Inc.

LITERATUURKOPIEEN
p. 1049-61

XP-002104523

Iron Chelation Decreases NF-κB and HIV Type 1 Activation due to Oxidative Stress

CHRISTINE SAPPEY,[1,2] JOHAN R. BOELAERT,[3] SYLVIE LEGRAND-POELS,[1] CHRISTINE FORCEILLE,[1] ALAIN FAVIER,[2] and JACQUES PIETTE[1]

ABSTRACT

An important aspect of human immunodeficiency virus (HIV-1) infection is the regulation of its expression by nuclear factor κB (NF-κB) through redox-controlled signal transduction pathways. In this study, we demonstrate that iron chelation by deferoxamine (DFO) protects against the cytotoxic and reactivating effects of hydrogen peroxide (H_2O_2). These protective effects were observed both in lymphocytic (ACH-2) and promonocytic (U1) cells latently infected by HIV-1. Concomitantly, NF-κB activation by H_2O_2, when followed by gel retardation assay, was decreased in the DFO-treated U1 and ACH-2 cells. This latter DFO-mediated effect was specific, as DFO did not clearly affect AP-1 DNA-binding activity when studied after H_2O_2-induced stress. More importantly, DFO protected against the H_2O_2-induced activation of HIV-1 as evidenced by reverse transcriptase activity in the supernatant. DFO also protected against PMA-induced NF-κB activation as well as TNF-α-induced HIV-1 activation. Furthermore, DFO attenuated the p24 response in PBMC infected with HIV-1 and stimulated with IL-2. These different effects of DFO were obtained at DFO concentrations lower than 5 μM. Other chemically unrelated iron chelators also provided protection against cytotoxicity, NF-κB activation, and HIV-1 activation in U1 cells challenged with H_2O_2.

INTRODUCTION

Immunodeficiency caused by the human immunodeficiency virus type 1 (HIV-1) is a multiphasic and multifactorial disease[1] that is the result of a systemic process that begins at the time of primary infection. This disease is characterized by a prolonged period of clinical latency that contributes to the propagation of HIV infection and to immune dysregulation.[2] Studies from several laboratories indicate that HIV-1 gene expression can be controlled by intracellular transduction pathways that are redox-regulated, implying that oxidative stress conditions may play an important role in the pathogenesis of AIDS.[3,4] This conclusion is supported by the observation that (1) HIV-1 infected individuals have abnormally low levels of antioxidant defenses[5,6] and (2) HIV-1 gene activation and virus replication in human T cells can be induced by reactive oxygen species (ROS) such as hydrogen peroxide (H_2O_2).[7,8] Moreover, HIV-1 activation mediated by ROS can be reduced *in vitro* by antioxidants such as *N*-acetyl-L-cysteine (NAC),[9,10] which replenish the intracellular level of reduced glutathione (GSH) and by selenium supplementation, which stimulates glutathione peroxidase activity.[11] The intracellular GSH concentration in T cells seems to constitute the central mechanism for modulating responses elicited by antigens and cytokines.[12] At high GSH concentrations, proliferation and mitogenic stimulations will be favored, whereas at low GSH concentrations, inflammatory-type responses that involve the induction of transcription factor NF-κB are more likely to occur.[13] These GSH-regulated functional differences could underlie major aspects of HIV-1 infection. Such patients tend to have low levels of extracellular thiols,[14] substantial decreases in median intracellular GSH levels in both $CD4^+$ and $CD8^+$ T cells,[15] and increased apoptotic activity.[16]

Because HIV-1 utilizes normal intracellular signaling pathways to regulate its expression, considerable interest has recently been focused on the role that selected host transcriptional factors may play in its initial activation by interacting with the long terminal repeat (LTR) of the integrated provirus.[17]

[1]Laboratory of Virology, Institute of Pathology B23, University of Liège, B-4000 Liège, Belgium.
[2]GREPO (Research Group on Oxidative Diseases), UFR Pharmacy, University of Grenoble, F-38000 Grenoble, France.
[3]Unit of Renal and Infectious Diseases, Algemeen Ziekenhuis Sint-Jan, B-8000 Brugge, Belgium.

ENSUUID: <XP___2104523A_1_>

12. Juli 2004 14:50 Lee & Stigter Nr. 0819 P. 5

Transcriptional activation of the LTR largely depends on a major enhancer made up of two directly repeated sequences able to respond to the transcription factor NF-κB.[17,18] For this DNA binding to occur and HIV-1 transcription to be initiated, NF-κB (usually associating p50 and p65 subunits) must be translocated into the nucleus from the cytoplasm, where it is normally retained by interaction with its inhibitory subunit, named IκB.[19,20] Functionally active NF-κB complexes are induced after cellular activation through the CD3-T cell receptor complex in T-lymphocytes, in response to antigen recognition[21,22] or following stimulation with other inducers such as phorbol esters, selected cytokines, or lipopolysaccharide in both lymphocytes and monocyte–macrophages.[23,24] Treatment of T-lymphocytes with H_2O_2 induces the nuclear appearance of NF-κB and its binding to DNA-responsive elements,[8] followed by a transcriptional activation of the proviral DNA in cells latently infected with HIV-1.[7]

Oxidative damage can be prevented, or at least minimized, by a variety of enzymatic and nonenzymatic defense systems.[25] Prominent among the former are superoxide dismutase and catalase, which scavenge O_2^- and H_2O_2, respectively.[25] Glutathione (GSH)-dependent selenoperoxidases reduce and detoxify H_2O_2 and a variety of organoperoxides, including lipid-derived species.[26] Iron also seems to play a central role in oxidative stress by being a catalyst of the superoxide-driven Haber–Weiss reaction, which generates hydroxyl radicals ($OH^·$).[27] The hydroxyl radical is a highly reactive radicalar species that abstracts hydrogen atoms from a large variety of biological molecules, initiating numerous damaging events such as lipid peroxidation[28] and damages to DNA involving base oxidation products or single-stranded breaks.[29] Thus, iron seems to serve as a catalyst for oxygen radical-driven $OH^·$ formation. In the case of polyunsaturated fatty acids, it can also account for initiating lipid peroxidation in the form of oxygen-bridged ferrous-ferric complexes.[28]

The present study was undertaken to determine whether ferric iron chelation can protect HIV-1 latently infected cells against activation initiated by an oxidative stress. Results described herein demonstrate that several iron chelators, even at low concentration, efficiently protect both lymphocytic and promonocytic cells against oxidative stress induced by H_2O_2. In addition, NF-κB activation and HIV-1 activation are decreased when oxidative stress is carried out in the presence of an iron chelator, demonstrating the role of iron in up-regulating HIV-1 expression under unbalanced redox conditions.

MATERIALS AND METHODS

Cell lines and culture conditions

The HIV-1 nonproductively infected T-lymphocytic cell line ACH-2, obtained from HIV-1 infected CEM-derived A3.01 cells, was cultivated in RPMI-1640 medium supplemented with 10% fetal calf serum (FCS), 100 U of penicillin per ml, and 100 μg of streptomycin per ml. The HIV-1 nonproductively infected promonocytic cell line U1, obtained from HIV-1 infected U397, was cultivated in the same medium as the ACH-2 cell line. Iron chelation was performed by adding the appropriate chelator to the culture medium 17 hr prior to the oxidative stress. Cell survival was determined by trypan blue exclusion. All experiments were performed in triplicate; in the Results section, one illustrative example is given for each experiment.

Peripheral blood mononuclear cells (PBMC) and virus isolation

Donor PMBC were prepared by Ficoll-Paque (Pharmacia, Sweden) density gradient centrifugation of heparinized blood from HIV-1 seronegative individuals. PMBC suspended to 2×10^6/ml in RPMI-1640 Glutamax-I (Gibco, USA) supplemented with 20% heat-inactivated fetal bovine serum and antibiotics were stimulated with phytohemagglutinin (PHA-P, Difco, USA) at 5 μg/ml for 3 days.

Two different clinical isolates were used: the first clinical HIV-1 isolate was obtained by cocultivation of PHA-stimulated donor PBMC with fresh PBMC from an infected individual. The culture was expanded and the virus stock frozen in aliquots at −70°C. This isolate turned out to be non-syncytia-inducing. The second HIV-1 isolate was syncytia-inducing and was obtained by cocultivation of a MT2-$CD4^+$ T-lymphocytic cell line with fresh PBMC from an infected individual.

Drug susceptibility assay

PBMC were cultivated in RPMI-1640 glutamax I supplemented with antibiotics, 20% heat-inactivated fetal bovine serum, and 10 IU/ml human recombinant interleukin-2 (Boerhinger, Germany). The titer of the virus stock was determined by endpoint dilution using 4-fold dilutions as previously described.[30] PBMC infection was performed as described in the standardized ACTG DOD HIV-1 drug susceptibility assay.[30] In brief, a standardized inoculum (10^5 $TCID_{50}$/1 × 10^6 PBMC) of virus and donor PBMC (2×10^6/ml) was incubated for 60 min, then unadsorbed viruses were removed by washing. The infected PBMC were resuspended at 1×10^6/ml and 1 ml of cell was aliquoted in a 24-well plate without or with DFO at 5 or 10 μM in final concentration. Experiments were carried out six times. PBMC cultivation was carried out at 37°C in humidified air with 5% CO_2. On day 3, one-half of the supernatant was removed and replaced with fresh medium. On day 7, the supernatants were collected and kept at −20°C for quantitative p24 antigen determination by ELISA (Coulter Immunology, USA). A 24-well control plate with the samples ×6 was included, using noninfected donor PBMC and DFO at the same final concentrations. This plate allowed us to determine DFO-induced cytotoxicity.

Chemicals

All the chemicals used were analytical grade reagents obtained from UCB (Brussels, Belgium). Deferoxamine (stock solution in water 380 mM) was obtained from Ciba-Geigy (Basel, Switzerland); *N,N'*-Bis(2-hydroxybenzyl)-ethylenediamine-*N,N'*-diacetic acid (HBED)[31] (stock solution in water 2.5 mM) was obtained from Dr. R.W. Grady (Department of Pediatrics, Cornell Medical Center, New York, NY); two 3-hydroxypyridin-4-one derivatives[32] were studied: CP20 (=L1), the 1,2-dimethyl derivative (stock solution in water 7.2 mM) was obtained from Duchefa (Haarlem, the Netherlands), and CP94, the 1,2-diethyl derivative (stock solution in water 6 mM) was

BNSDOCID: <XP___2104523A__1_>

12. Juli 2004 14:51 Lee & Stigter Nr. 0819 P. 6

obtained from Ciba-Geigy (Basel, Switzerland); two biomimetic "reversed" siderophores[33] derived from ferrichrome were generously provided by Prof. A. Shanzer (Weizmann Institute, Rehovot, Israel): RSF-leu and RSF-ileu (stock solution in DMSO both at 322 mM). DMSO at concentrations lower than 5 μM did not interfere with the effects of H_2O_2.

Exposure of ACH-2 and U1 cells to H_2O_2

ACH 2 or U1 cells, at 6×10^6 in 7.5 ml culture medium, were cultivated in 25-cm^2 culture flasks containing the studied iron chelators. Seventeen hours later, H_2O_2 was added at different concentrations (from 0 to 300 μM for ACH-2 and from 0 to 5 mM for U1). Cells ($4–5 \times 10^6$) were harvested three hours later for NF-κB or AP-1 gel shift analysis. After 48 hr, ACH-2 and U1 cells were counted using trypan blue exclusion, and aliquots of supernatant corresponding to 0.25×10^6 cells were collected for reverse transcriptase (RT) activity determination.

Reverse transcriptase (RT) assay

The RT assay was done as previously described.[34] Briefly, the virus was purified and concentrated by ultracentrifugation of supernatant fluids (131,000*g* at 4°C for 120 min). Pellets were resuspended in 25 μl of TNE (10 mM Tris-HCl, 100 mM NaCl, 1 mM EDTA) containing 0.1% Triton X-100 and left for 30 min on ice. Then 10 μl of the virus preparation was incubated at 37°C for 60 to 90 min with 40 μl of a solution containing 62.5 mM Tris-HCl pH 7.8, 6.25 mM dithiothreitol, 6.25 mM $MgCl_2$, 180 mM KCl, 0.06% Triton X-100, 0.375 mM glutathione, 0.325 mM EGTA, 31 μg/ml BSA, 2.5% ethylene glycol, 250 mU/ml poly(rA)-oligo(dT) and 125 mCi/ml [^{3}H]deoxythymidine. The resulting DNA was precipitated with 10% trichloroacetic acid (TCA) and filtered through 2.4-mm Whatman GF-A filters. Filters were rinsed with 0.01 M sodium pyrophosphate, dried with 95% ethanol, and then counted by liquid scintillation (LKB Minibeta, Sweden).

Electrophoretic mobility shift assay

Oligonucleotides used for the electrophoretic mobility shift assays encompassed either the NF-κB sites of the HIV-1 enhancer or the AP-1 sites of the collagene type 1 promoter. They were labeled by end-filling with the Klenow fragment of *E. coli* DNA polymerase (Boehringer, Germany) with [^{32}P]dATP, [^{32}P]dCTP (New England Nuclear, UK), and cold dTTP + dGTP. Labeled probes were purified by spin chromatography on G-25 columns. Nuclear extracts were isolated as described by a rapid micropreparation technique based on the use of a hypotonic lysis followed by high salt extraction of nuclei.[35] This procedure was derived from the large-scale procedure of Dignam *et al.*[36] Binding of nuclear proteins to the oligonucleotide probes was performed for 25 min at room temperature with 3–5 μg total protein in 10–20 μl of 20 mM HEPES-KOH (pH 7.9), 75 mM NaCl, 1 mM EDTA, 5% glycerol, 0.5 mM $MgCl_2$, 1 μg acetylated bovine serum albumin, 1.5 μg poly(dI-dC)–poly(dI-dC) (Pharmacia, UK), 1 mM DTT, and 0.2 ng of ^{32}P-labeled oligonucleotides (Eurogentec, Belgium). DNA-nuclear protein complexes were separated from unbound probes on native 6% polyacrylamide gels at 150 mV in 0.25 M Tris, 0.25 M $Na_2B_4O_7$, and 0.5 mM EDTA at pH 8.0. Gels were vacuum-dried and exposed to Fuji X-ray films at −80°C for 16 to 24 hr. The amounts of specific complexes were determined by measuring the radioactivity with a phosphorimager (Molecular Dynamics, USA). The probes have the following sequences: Wild-type NF-κB probe: 5′-GATCAGGGACTTTCCGCTGGGGACTTTCCAG-3′ 3′-TCCCTGAAAGGCGACCCCTGAAAGGTCCTAG-5′ Wild-type AP-1 probe: 5′-CTAGAGGTGTCTGACTCATGCTTA-3′ 3′-TCCACAGACTGAGTACGAATTCGA-5′.

RESULTS

Iron chelation by deferoxamine (DFO) protects U1 and ACH-2 cells against the cytotoxic effect induced by H_2O_2

U1 and ACH-2 cells were grown for 17 hr in the presence of various DFO concentrations before being exposed to different H_2O_2 concentrations. In the case of U1 cells, H_2O_2 concentrations ranged from 0 to 5 mM, whereas in the case of ACH-2 cells the concentration range was between 0 and 300 μM. Forty-eight hours after the oxidative stress, cell survival was determined by trypan blue exclusion. As shown in Figure 1A and 1C, H_2O_2 caused a significant reduction in cell survival as compared to untreated cells. Cells grown in the presence of increasing DFO concentrations (from 0 to 5 μM) exhibited a concentration-related protection against the oxidative stress caused by H_2O_2. Even at a DFO concentration as low as 2–2.5 μM (Fig. 1A and C), DFO completely eliminated the cytotoxic effect throughout a wide range of H_2O_2 concentrations (up to 5 mM in the case of U1 cells). In the absence of H_2O_2, DFO at concentrations lower than 5 and 10 μM was devoid of any cytotoxic effect on ACH-2 and U1 cells, respectively (data not shown).

The involvement of iron chelation in the protective effect induced by DFO was demonstrated by addition of various amount of Fe^{3+} ($FeCl_3$ or Fe-nitriloacetic acid) to the DFO-treated U1 cells. Increasing concentrations of Fe^{3+} (5, 10, or 20 μM) reestablished the cytotoxic effect induced by H_2O_2 (Fig. 1B). Similar observations were made with ACH-2 cells (data not shown), demonstrating that iron plays a central role in the cytotoxic effect induced by oxidative stress in HIV-1 latently infected cells.

Iron chelation by DFO protects U1 and ACH-2 cells against HIV-1 activation induced by H_2O_2

We have previously demonstrated[7] that oxidative stress induced by H_2O_2 activates HIV-1 replication in both ACH-2 and U1 cells, as measured by the appearance of reverse transcriptase (RT) activity in cell supernatants. U1 and ACH-2 cells were grown for 17 hr in the presence of DFO (as described above) before being stressed by various concentrations of H_2O_2. RT activities were determined in cell supernatants after 48 hr of stress. As shown in Figure 2A and C, RT stimulation was proportional to the H_2O_2 concentration: e.g., at 3 mM H_2O_2, RT activity was stimulated approximately 20-fold in U1 cells and 6-fold in ACH-2 cells at 100 μM H_2O_2. After DFO supplementation, HIV-1 activation by H_2O_2 was strongly diminished; it was completely abolished at DFO concentrations as low as

ENSUCCID: <XP___2104523A__1_>

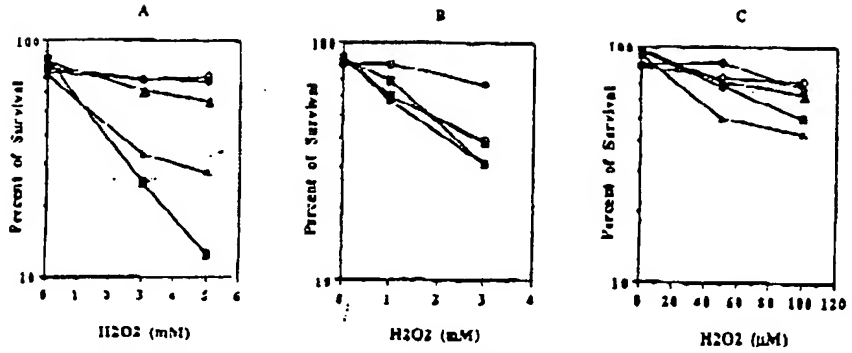

FIG. 1. Iron chelation by desferrioxamine (DFO) inhibits cytotoxic effects in HIV-1 latently infected cells treated with H_2O_2. Cytotoxic effect was measured 48 hr after the oxidative stress. Relative errors were estimated to be ±10%. (A) U1 cells were supplemented with several DFO concentrations (■, 0; Δ, 1.25; ▲, 2.5; O, 3.75; and ●, 5 μM) for 17 hr before being exposed to H_2O_2; 48 hr after the stress, cells were counted by trypan blue exclusion. Percentage of survival (log_{10}) is plotted vs H_2O_2 concentrations (in mM). (B) U1 cells were treated with DFO at 5 μM plus several Fe^{3+} concentrations (□, Fe^{3+} 5 μM; O, Fe^{3+} 10 μM; Δ, Fe^{3+} 20 μM). Controls where U1 cells were treated only with H_2O_2 are shown by ■ or by H_2O_2 and 5 μM DFO by ●. (C) ACH-2 cells were supplemented with several DFO concentrations (■, 0; Δ, 0.25; ▲, 0.5; O, 1; and ●, 2 μM) for 17 hr before being exposed to H_2O_2; 48 hr after the stress, cells were counted by trypan blue exclusion. Percentage of survival (log_{10}) is plotted vs H_2O_2 concentrations (in μM).

3.75 and 5 μM (Fig. 2A) while only a very weak activation could be detected at 5 mM H_2O_2 in the presence of 2.5 μM DFO in U1 cells (Fig. 2A). Similar observations were made with ACH-2 cells (Fig. 2C): DFO provided a substantial protection against HIV-1 activation whatever the H_2O_2 concentration used. In addition, it should be mentioned that DFO at concentrations lower than 5 and 10 μM was devoid, in the absence of H_2O_2, of any reactivating effect on ACH-2 and U1 cells, respectively.

Involvement of iron in the protection induced by DFO was demonstrated by addition of iron ($FeCl_3$ or Fe-nitriloacetic acid) to the U1 cells treated with DFO. The activation effect was progressively restored by adding increasing concentrations of iron to the DFO-treated cells (Fig. 2B). This demonstrates the central role of iron in HIV-1 activation induced by oxidative stress.

These data obtained with nonproductively infected monocytes or lymphocytes were extended using fresh PBMC infected with two clinical HIV-1 isolates, one syncytia-inducing and the other non-syncytia-inducing. Infected PBMC were cultivated for 7 days in the presence of human interleukin 2 without or with DFO (at 5 or 10 μM). After cultivation, p24 antigen was measured in cell supernatants. Six independent measurements were performed per DFO concentration. As shown in Table 1, DFO at 5 μM markedly decreased the amount of p24 antigen produced by the two HIV-1 isolates tested. A higher DFO con-

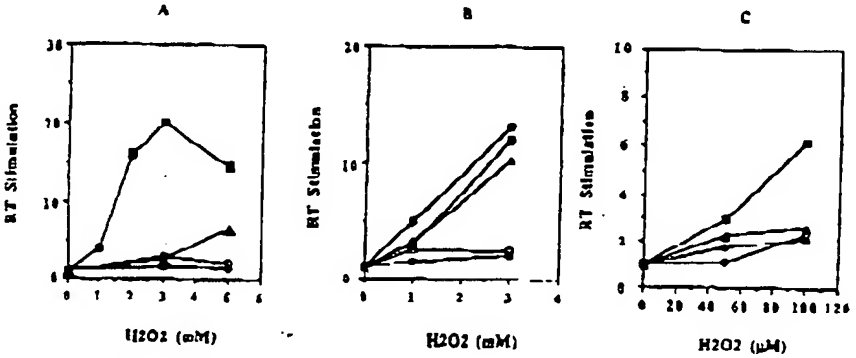

FIG. 2. Iron chelation by DFO inhibits HTV-1 activation in HIV-1 latently-infected cells mediated by H_2O_2. Supernatants, corresponding to an identical cell count, were taken 48 hr after the reaction to determine reverse transcriptase (RT) activities. The stimulation of RT activity is the ratio of the activity at the various time points to the initial RT value. Stimulation of RT is plotted vs H_2O_2 concentrations (relative errors were estimated to be ±10%). (A) U1 cells were supplemented with various DFO concentrations (■, 0; ▲, 2.5; O, 3.75; and ●, 5 μM) for 17 hr before being exposed to H_2O_2. (B) U1 cells were loaded with several Fe^{3+} concentrations (□, Fe^{3+} 5 μM; O, Fe^{3+} 10 μM; Δ, Fe^{3+} 20 μM) and treated with DFO at 5 μM. Controls where U1 cells were treated only with H_2O_2 are shown by ■ or with H_2O_2 and 5 μM DFO by ●. (C) ACH-2 cells were supplemented with several DFO concentrations (■, 0; ▲, 0.5; O, 1; and ●, 2 μM) for 17 hr before being exposed to H_2O_2.

TABLE 1. EFFECT OF DFO ON p24 ANTIGEN PRODUCTION 7 DAYS AFTER INFECTION OF PBMC WITH EITHER A SYNCYTIA-INDUCING HIV-1 ISOLATE (SI) OR A NON-SYNCYTIA-INDUCING ISOLATE (NSI)

		p24 antigen (ng/ml)[a]	
DFO (μM)	Cell concentration (× 10^6)	HIV-1 (NSI) isolate	HIV-1 (SI) isolate
0	4.48 ± 0.33	449.9 ± 21.9	381.3 ± 76.1
5	3.55 ± 0.84	241.9 ± 42.1	232.9 ± 15.3
10	2.35 ± 0.48	57.8 ± 37.1	89.5 ± 39.3

[a]Mean of six independent cultures (mean ± SD).

centration (10 μM) gave rise to an even higher inhibition, indicating that expression of p24 antigen is reduced in a dose-dependent manner. These data on p24 assay confirm the results obtained with RT activity in both U1 and ACH-2 cell lines.

Iron chelation by DFO decreases NF-κB activation induced by H_2O_2

Because DFO supplementation leads to iron chelation and protects U1 and ACH-2 cells against both the cytotoxic and activating effects of H_2O_2, we tested whether this supplementation also affects the activation of NF-κB. Nuclear protein ex-

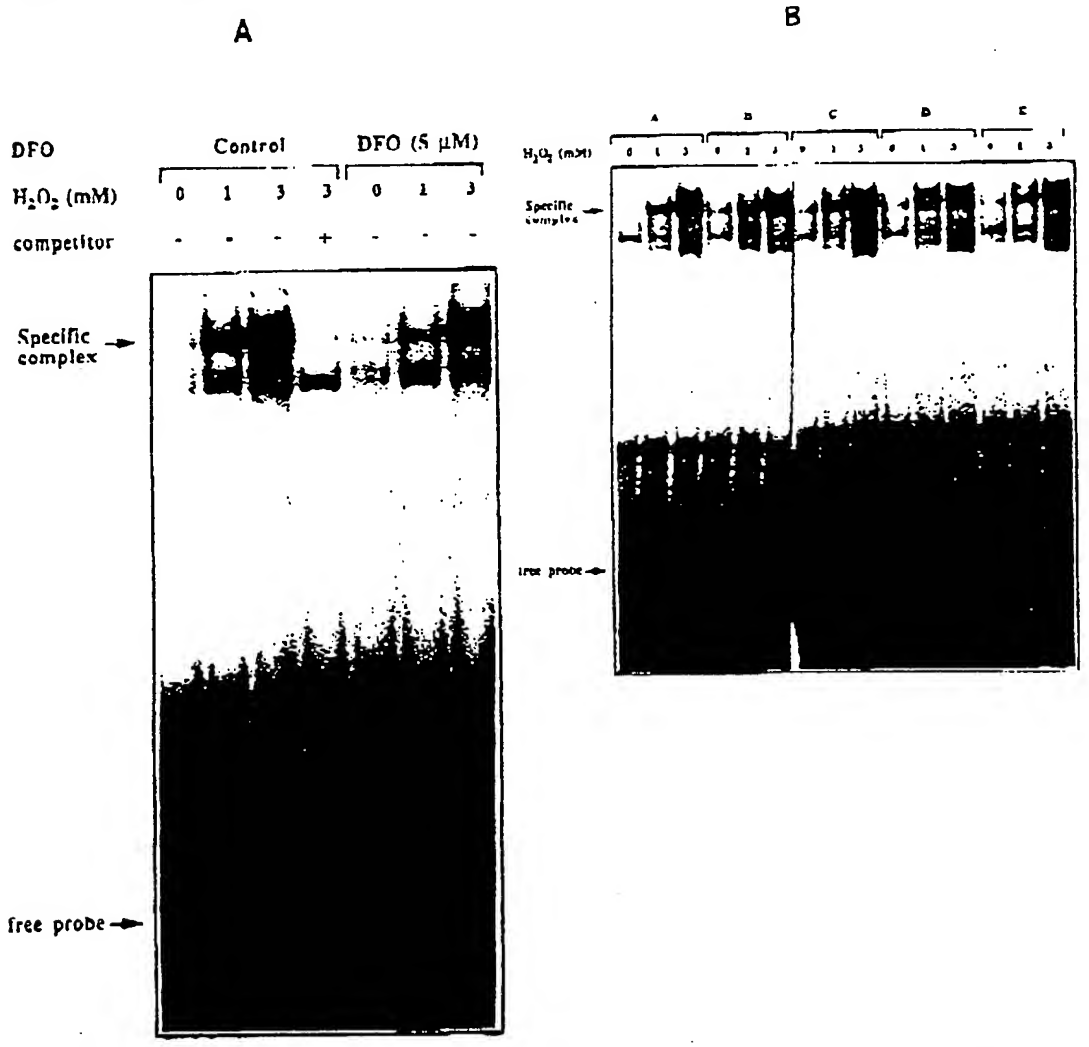

FIG. 3. Effect of ferric iron chelation by DFO on NF-κB DNA-binding activity in U1 cells induced by H_2O_2. Rapid induction of a nuclear κB enhancer DNA-binding protein by treatment of U1 cells with increasing concentrations of H_2O_2. Nuclear extracts were prepared 180 min after the reaction with equal amounts of proteins and mixed with a ^{32}P-labeled probe encompassing the κB elements of the HIV-1 enhancer. Samples were loaded on 6% native polyacrylamide gels and electrophoresed at 150 V. Autoradiogram of the gel is shown. Arrows indicate the position of the specific complex and of the free probe. Competition with an unlabeled oligonucleotide encompassing NF-κB sites visualizes the position of the specific NF-κB complex. (A) U1 cells were supplemented with 0 or 5 μM DFO before being stressed by 0, 1, or 3 mM H_2O_2. (B) U1 cells were supplemented with 0 or 5 μM DFO or loaded with increasing concentrations of Fe^{3+} before being stressed by 0, 1, or 3 mM H_2O_2. A, in the absence of DFO; B, DFO (5 μM); C, DFO (5 μM) plus Fe^{3+} (5 μM); D, DFO (5 μM) plus Fe^{3+} (10 μM); and E, DFO (5 μM) plus Fe^{3+} (20 μM).

12. Juli 2004 14:53 Lee & Stigter Nr. 0819 P. 9

tracts were prepared from U1 or ACH-2 cells supplemented with various DFO concentrations and subsequently treated by H_2O_2. Nuclear protein extracts prepared 3 hr after the stress were analyzed by gel shift assay, and the NF-κB specific complexes were quantified using a phosphorimager. As shown in Figure 3A, a 1 mM concentration of H_2O_2 was sufficient to cause the appearance of the NF-κB retardation complex in the U1 cell nucleus; the induction seemed to be optimal at 3 mM H_2O_2. This retarded band completely disappeared when the nuclear extracts obtained after reaction with 3 mM H_2O_2 were mixed with an excess of unlabeled oligonucleotide encompassing the NF-κB sites of the HIV-1 enhancer (Fig. 3A, lane 4). This competition experiment demonstrated that the most retarded band (shown by an arrow on Fig. 3A) corresponded to the specific NF-κB complex. As shown in Figure 3A, the intensity of the specific NF-κB band was decreased when U1 cells were supplemented with 5 μM of DFO and stressed with either 1 or 3 mM H_2O_2 (lanes 6 and 7, respectively). The demonstration that iron chelation was involved in the decrease of NF-κB induction was carried out by adding iron ($FeCl_3$ or Fe-nitriloacetic acid) to the DFO treated cells. Indeed, the addition of increasing concentrations of iron to these cells led to the reappearance of NF-κB in the nucleus of the U1 cells treated with H_2O_2 (Fig. 3B, lanes 7 to 15). Controls involving untreated cells, cells treated with H_2O_2 alone, and with H_2O_2 and DFO are shown in Figure 3B.

A similar induction of the specific NF κB complex was observed when ACH-2 cells were treated with 100 to 300 μM H_2O_2 (Fig. 4A, lanes 2, 3, and 5); an 8-fold stimulation was obtained with 300 μM H_2O_2. Conversely, DFO supplementation decreased the level of NF-κB induction in the nucleus of ACH-2 cells (Fig. 4A, lanes 6 to 13). Competition experiments carried out with an unlabeled NF-κB probe demonstrated that the observed retarded band corresponded to the appearance of a specific NF-κB complex (Fig. 4A, lane 4). Measurement of the intensity of the NF-κB bands indicated a maximum induction of the NF-κB complex at 300 μM H_2O_2 (Fig. 4B). At this H_2O_2 concentration, both 2 and 4 μM of DFO resulted in an important inhibition of the NF-κB complex (up to 50%). At lower H_2O_2 concentrations, NF-κB induction was not as great although the protective effect induced by DFO was still clearly detectable (Fig. 4B).

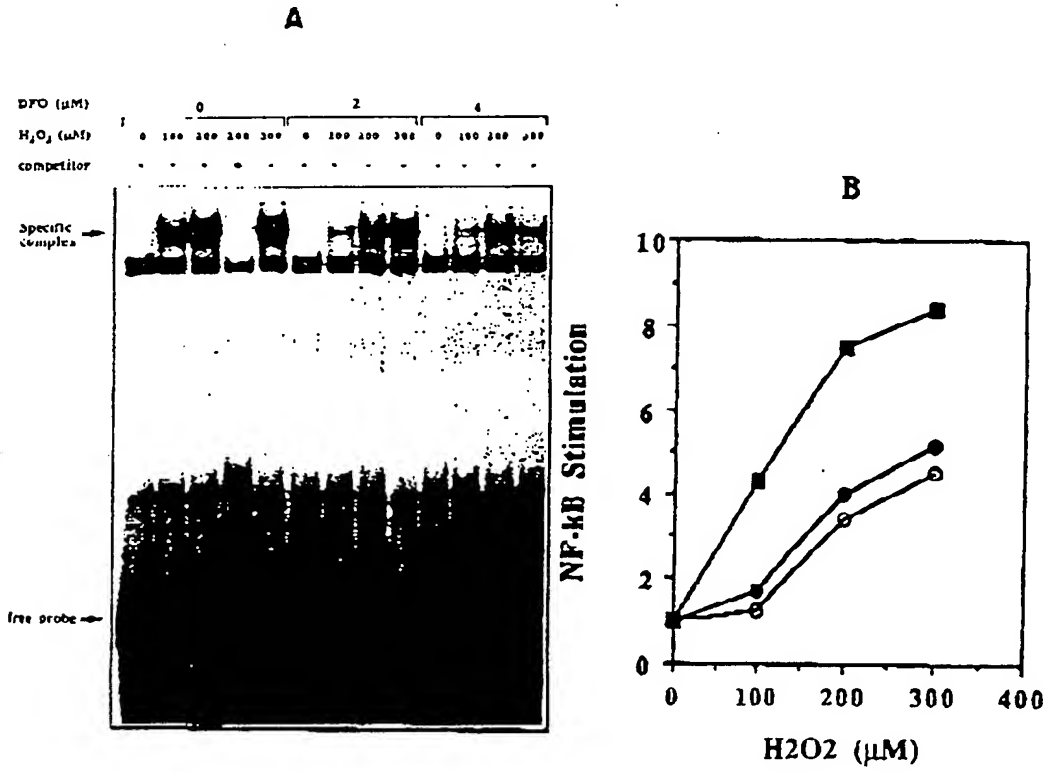

FIG. 4. (A) Effect of ferric iron chelation by DFO on NF-κB DNA-binding activity in ACH-2 cells induced by H_2O_2. Rapid induction of a nuclear κB enhancer DNA-binding protein by treatment of ACH-2 cells with increasing concentrations of H_2O_2. Nuclear extracts were prepared 180 min after the reaction with equal amounts of proteins and mixed with a ^{32}P-labeled probe encompassing the κB elements of the HIV-1 enhancer. Arrows indicate the position of the specific complex and of the free probe. Competition with an unlabeled oligonucleotide encompassing NF-κB sites visualizes the position of the specific NF-κB complex. Cells were supplemented with either 0, 2, or 4 μM DFO before being stressed by 0, 100, 200, or 300 μM H_2O_2. (B) Stimulation of NF-κB DNA-binding activities detected in the nucleus of ACH-2 cells plotted vs H_2O_2 concentrations. Cells were supplemented with various DFO concentrations: ■, 0 μM; ●, 2 μM; ○, 4 μM.

RNSOOCID: <XP__2104523A 1 >

12. Juli 2004 14:53 Los & Stigler Nr. 0819 P. 10

DFO supplementation does not strongly affect AP-1 induction by H_2O_2

AP-1 is another transcription factor that has been shown to be less induced in T-lymphocytes or in monocytes by H_2O_2,[8] although it has also been characterized as a secondary antioxidant-responsive factor.[37] To test possible AP-1 activity as an antioxidant-responsive factor, U1 cells were supplemented with DFO (from 0 to 5 μM) before being treated with H_2O_2. Nuclear cell extracts were prepared at 180 min after induction of the stress. As shown in Figure 5, a weak retarded band could be detected in untreated U1 cells; the intensity of this band was increased after reaction with 1 and 3 mM H_2O_2 (lanes 2 and 3). Competition with unlabeled oligonucleotide encompassing AP-1 sites strongly decreased the intensity of the most retarded band, demonstrating that this band was due to a specific AP-1

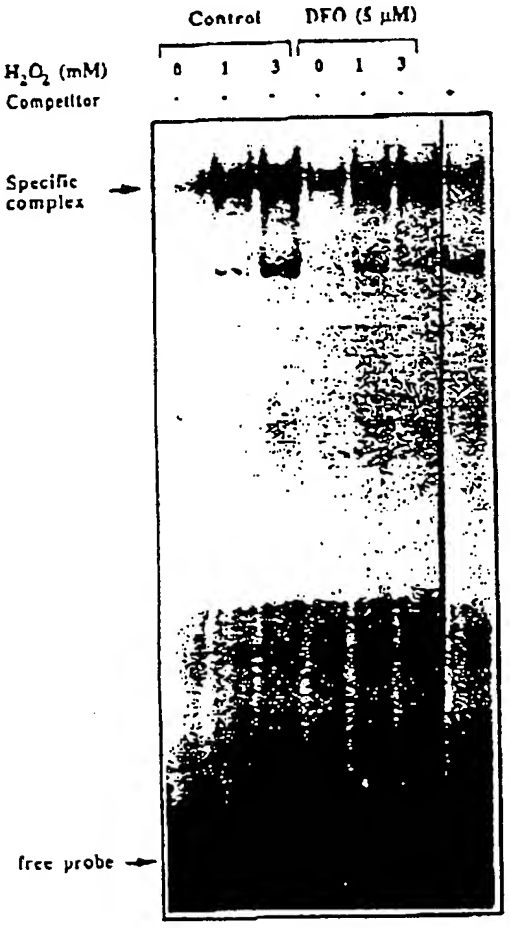

FIG. 5. AP-1 DNA-binding activities in U1 cells supplemented with DFO and treated with H_2O_2. Nuclear extracts were prepared 3 hr after the reaction and mixed with a ^{32}P labeled probe encompassing the TRE elements of the type I collagenase promoter before being loaded on a native polyacrylamide gel as described in Figure 3. Gel shift assays show the separation of specific AP-1 complexes from the free probe. U1 cells supplemented with 5 μM DFO were treated with various H_2O_2 concentrations (0 or 3 mM).

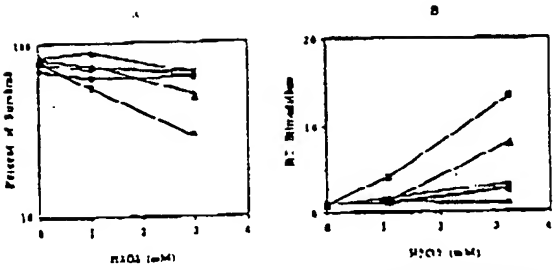

FIG. 6. (A) Iron chelation by various chelators inhibits cytotoxic effects in U1 cells treated with H_2O_2. Cytotoxic effect was measured 48 hr after the oxidative stress. U1 cells were supplemented with several iron chelators [■, none; ▲, RSF-leu (5 μM); O, CP94 (60 μM); +, L1 (60 μM); △, RSF-ileu (5 μM); □, HBED (20 μM)] for 17 hr before being exposed to H_2O_2; 48 hr after the stress, cells were counted by trypan blue exclusion. Percentage of survival (log_{10}) is plotted vs H_2O_2 concentrations (in mM). Relative errors were estimated to be ±10%. (B) Iron chelation by various chelators inhibits HIV-1 activation induced by H_2O_2 in U1 cells. Supernatants, corresponding to an identical cell count, were taken 48 hr after the reaction to determine RT activities. The stimulation of RT activity is the ratio of the activity at the various time points to the initial RT value. Stimulation of RT is plotted vs H_2O_2 concentrations. U1 cells were supplemented with several iron chelators [■, none; ▲, RSF-leu (5 μM); O, CP94 (60 μM); +, L1 (60 μM); △, RSF-ileu (5 μM); □, HBED (20 μM)] for 17 hr before being exposed to H_2O_2. Relative errors were estimated to be ±10%.

complex (lane 7). DFO supplementation did not modify the amount of AP-1 complex in untreated cells (Fig. 5, lane 4) but led to a slight protective effect against the oxidative stress induced by H_2O_2 (Fig. 5, lanes 5 and 6). Quantitative analysis of the amount of AP-1 complex induced by 1 mM H_2O_2 in the absence or in the presence of DFO disclosed a 2.5-fold and 1.7-fold stimulation, respectively, confirming that the inducibility of AP-1 in U1 cells is less influenced by unbalanced redox conditions than that of NF-κB.

Other iron chelators also protect U1 cells against cytotoxicity, NF-κB activation and HIV-1 activation induced by H_2O_2

Several iron chelators other than DFO were studied using the same systems as described above: i.e., latently infected U1 cells as substrate and H_2O_2 as a reactivating event. The studied iron chelators were HBED, a mixed phenolate and aminocarboxylate derivative; L1 and CP94, which are hydroxypyridone compounds; and RSF-leu and RSF-ileu, which are synthetic ferrichrome derivatives. These different chelators were mixed individually with U1 cells 17 hr prior to an oxidative stress induced by H_2O_2. So that these compounds could be compared to DFO, they were supplemented to the cells at equivalent iron chelating concentrations, taking their different stoichiometric properties into account (1 to 1 stoichiometry for DFO, HBED, RSF-leu, and RSF-ileu; 1 to 3 iron to ligand stoichiometry for CP94 and L1). At the indicated concentration, only RSF-ileu gave rise to a protective effect, which was largely comparable to that observed with DFO at similar H_2O_2 concentrations (Fig.

12. Juli 2004 14:54 Los & Stigler Nr. 0819 P. 11

6A); RSF-leu was somewhat less efficient, whereas HBED, L1, and CP94 were not protective when added to U1 cells at the same stoichiometric concentration as DFO (data not shown). HBED was then tested over a wider range of concentrations (from 0 to 100 μM) to determine whether or not this compound could protect against the cytotoxic effect of H_2O_2. At 20 μM, HBED resulted in protection from cytotoxicity (Fig. 6A). CP94 and L1 were tested at an equivalent iron binding concentration (60 μM) as 20 μM HBED: at this concentration, both hydroxypyridone compounds protected against H_2O_2 cytotoxicity (Fig. 6A).

U1 cells treated under these experimental conditions were brought back in culture at 37°C before measuring HIV-1 activation by assaying RT in the cell supernatants. When supplemented at the indicated concentrations, the various iron chelators exhibited a protective effect against HIV-1 activation (Fig. 6B), as evidenced by the low or non-existent RT activity in the cell supernatants (Fig. 6B).

Nuclear cell extracts were prepared 3 hr after the oxidative stress induced by H_2O_2 to visualize NF-κB activation by gel retardation assay. As shown in Figure 7, the retarded band corresponding to the NF-κB-specific complex induced in the nucleus of U1 cells by 3 mM H_2O_2 was induced to a lesser extent when cells were treated with RSF-ileu (Fig. 7, lanes 11 and 12). HBED (lanes 14 and 15), CP94 (lanes 17, 18), and L1 (lanes 20 and 21). At a similar concentration (5 μM), RSL-leu was less protective than RSF-ileu (Fig. 7, lanes 8 and 9). Addition of Fe-NTA to U1 cells pretreated with these chelators restored the initial effects of H_2O_2, demonstrating that these compounds acted through iron chelation (data not shown).

Effects of DFO and RSF-ileu on induction by TNF-α

NF-κB has been shown to be induced by a wide variety of agents; among them, TNF-α is one of the most efficient. U1 or ACH-2 cells supplemented with DFO (2.5 or 5 μM) were treated with TNF-α (0 to 200 U/ml) for 120 min. After induction, nuclear extracts were prepared and analyzed by gel retardation assay. As shown in Figure 8A, a specific NF-κB complex could be clearly detected, even at TNF-α concentrations as low as 20 U/ml. At 200 U of TNF-α/ml, NF-κB was stimulated ca. 4-fold. At higher TNF-α concentrations, the degree of stimulation slightly decreased. In U1 cells treated with DFO at 5 μM, NF-κB induction by TNF-α was not clearly modified (Fig. 8A). The same result was observed with ACH-2 cells treated under similar conditions: NF-κB inducibility by TNF-α did not seem to be affected by DFO (Fig. 8B). Among the other iron chelators tested above, it turned out that RSF-ileu was the most effective. We therefore investigated the effects of this iron chelator on NF-κB induction by TNF-α. Similar to

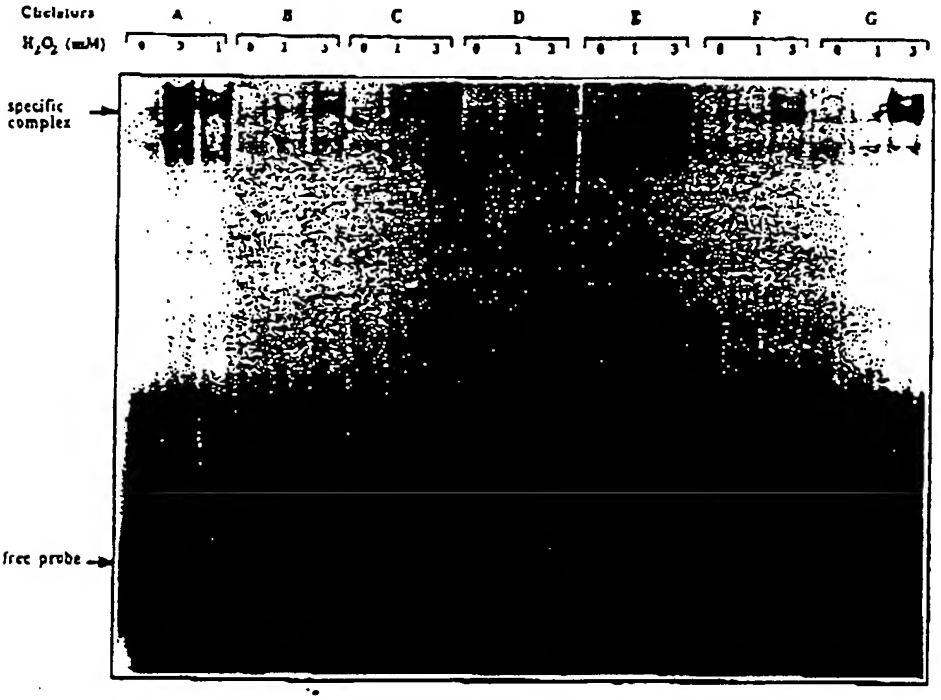

FIG. 7. Effect of various iron chelators on NF-κB DNA-binding activity in U1 cells induced by H_2O_2. Rapid induction of a nuclear κB enhancer DNA-binding protein by treatment of U1 cells with increasing concentrations of H_2O_2 (0, 1, and 3 mM). Nuclear extracts were prepared 180 min after the reaction with equal amounts of proteins and mixed with a ^{32}P-labeled probe encompassing the κB elements of the HIV-1 enhancer. Samples were loaded on 6% native polyacrylamide gels and electrophoresed at 150 V. Autoradiogram of the gel is shown. Arrows indicate the position of the specific complex and of the free probe. (A) In the absence of chelator; (B) DFO (5 μM). (C) RSF-leu (5 μM); (D) RSF-ileu (5 μM); (E) HBED (20 μM); (F) CP94 (60 μM); and (G) L1 (60 μM).

ANSOOCID: <XP__21045238__1_>

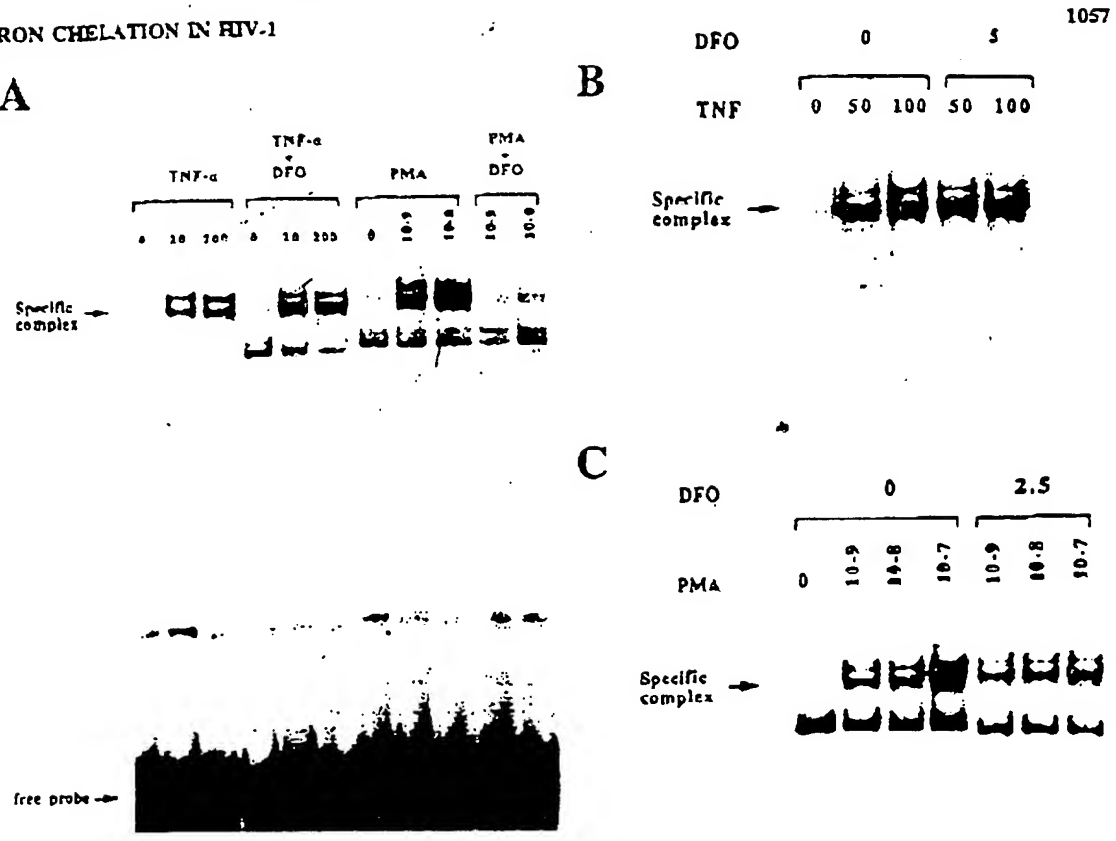

FIG. 8. Induction of a nuclear kB enhancer DNA-binding protein by treatment with TNF-a (A, B) or PMA (C, E). Nuclear extracts were prepared 120 min after the reaction with equal amounts of proteins and mixed with a ^{32}P-labeled probe encompassing the κB elements of the HIV-1 enhancer. Samples were loaded on 6% native polyacrylamide gels and electrophoresed at 150 V. Autoradiogram of the gel is shown. Arrows indicate the position of the specific complex and of the free probe. (A) Induction of a NF-κB DNA-binding activity in U1 cells induced by TNF-α (0, 20, and 200 U/ml) or by PMA (0, 10^{-9}, 10^{-8} M) in the absence or in the presence of DFO at 5 μM. (B) Effect of DFO at 5 μM on NF-κB DNA-binding activity in ACH-2 cells induced by TNF-α (0, 20, and 200 U/ml). The upper part of the gel is shown. (C) Effect of DFO at 2.5 μM on NF-κB DNA-binding activity in ACH-2 cells induced with PMA (10^{-9}, 10^{-8}, and 10^{-7} M). The upper part of the gel is shown.

what was observed with DFO. U1 cells supplementation with 5 μM RSF-ileu did not modify NF-κB inducibility by TNF-α concentration varying from 0 to 200 U/ml (data not shown).

On the other hand, RT measurements performed on U1 cells treated with either DFO or RSF-ileu at 5 μM and induced with 100 U/ml of TNF-α showed that iron chelation clearly reduces HIV-1 activation in these cells (Fig. 9). These data show that DFO and RSF-ileu at 5 μM prevent HIV-1 induction by TNF-α, even if the drugs do not strongly influence NF-κB induction. This suggests that in this setting, DFO and RSF-ileu may act primarily via inhibition of the cellular ribonucleotide reductase.[38]

Iron chelation by DFO decreases NF-κB activation induced by PMA

PMA is a potent NF-κB activator in a wide variety of cells such as T cells, monocytes, and HeLa cells. U1 or ACH-2 cells were grown in the presence or not of DFO before being induced by PMA, again for 120 min. Cell nuclear extracts were prepared and analyzed by gel retardation assay. The specific NF-κB retardation band was clearly detectable in both DFO-supplemented and DFO-unsupplemented cells treated with PMA. As shown in Figure 8A, the amount of NF-κB complex increased strongly when U1 cells were stimulated with PMA concentrations between 10^{-9} and 10^{-8} M. Compared with non-supplemented cells, the amount of NF-κB complex was significantly lower in DFO-treated cells induced with PMA at 10^{-9} and 10^{-8} M. The results of DFO supplementation using ACH-2 cells treated with PMA confirmed this result (Fig. 8C), indicating that NF-κB activation by PMA takes place through the generation of ROS.

DISCUSSION

HIV infection is characterized by a long clinical latency period between the time of infection and the onset of AIDS.[1] It is, however, suspected that fever, inflammation, or responses

12. Juli 2004 14:55 Lee & Stieler Nr. 0819 P. 13

of the immune system might play fundamental roles as activating factors,[1] leading to an increased production of ROS.[39] The demonstration that HIV can be activated by H_2O_2[7] through the activation of NF-κB[8] established a direct link between ROS and viral expression. These results justified interest in enzymatic and nonenzymatic antioxidants as possible means of extending the HIV latency period or, perhaps, as a new approach to anti-HIV therapy.[40] We used this concept as a guideline for our experiments dealing with HIV-1 latently infected T-lymphocytic and promonocytic cell lines and the chelation of iron.

Iron is essential to almost all known cell types. Many iron-requiring enzymes are involved in metabolic pathways important for the growth and development of cells[41] such as the clonal expansion of lymphocytes.[42,43] Iron not only participates in numerous important biological reactions,[44–46] but also plays a central role in oxidative stress, being a major catalyst of cellular hydroxyl radical formation.[27] For example, iron is involved in the Fenton reaction, in which ferrous iron acts as an electron donor to generate the hydroxyl radical through reduction of H_2O_2. Iron is a catalyst of the Haber–Weiss reaction, which consists of a one-electron transfer from superoxide to hydrogen peroxide.[27] Hydroxyl-free radicals generated by this and other mechanisms can in turn lead to numerous deleterious effects, including DNA damages[29] and lipid peroxidation.[28] The trihydroxamate iron chelator DFO causes both intracellular and extracellular iron depletion,[47,48] producing inhibition of cell proliferation[49] and inhibition of ribonucleotide reductase activity in lymphocytes with decreased availability for deoxyribonucleotides for DNA synthesis.[38] While ribonucleotide reductase may well be a primary site for action of iron chelators, other enzymes and metabolic pathways may also be affected and contribute to the biological effects induced by iron chelation. In addition to DFO, which has been used for decades, other molecules exhibit iron chelation properties. One of them, CP20 (L1), has been used in several hundreds of iron overloaded patients.[50] Hydroxamate derivatives have recently been used in conjunction with 2',3'-dideoxyinosine and showed very promising synergistic effects resulting in the total suppression of viral production, total protection against the cytopathic effect induced by viral replication, and no effect on the ability of the cells to replicate in cell culture.[51]

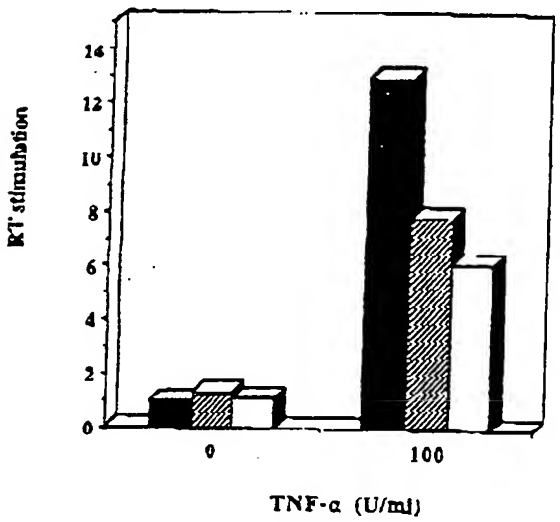

FIG. 9. Iron chelation by DFO (□) (5 μM) or by RSF-ileu (□) (5 μM) inhibits HIV-1 activation in U1 cells mediated by TNF-α (100 U/ml) (■). Supernatants, corresponding to an identical cell count, were taken 48 hr after the reaction to determine reverse transcriptase (RT) activities. The stimulation of RT activity is the ratio of the activity at 48 hr to the initial RT value (relative errors were estimated to be ±10%).

The present study indicates that iron plays a central role in triggering the deleterious effects of the oxidative stress induced by H_2O_2, PMA or TNF-α. Conversely, iron chelation by DFO or by several chemically unrelated chelators protects not only against the cytotoxic effect induced by H_2O_2, but also against NF-κB activation and HIV-1 activation in lymphocytes and monocytes latently infected by HIV-1. The present results are in agreement with various reports that implicate $OH^{\cdot}$ as the deleterious species in oxidative stress.[52] Hydroxyl radicals would then trigger, probably indirectly, activation of tyrosine kinases such as ZAP-70, $p56^{lck}$, and $p59^{fyn}$, and strong Ca^{2+} fluxes,[53–55] which would ultimately lead to the phosphorylation of the I-κB subunit or of the p105 precursor and their subsequent proteolysis, allowing p50 and p65 of NF-κB to migrate from the cytoplasm to the nucleus and to bind to the NF-κB responsive elements. Iron removal by DFO or by other iron chelators would impair this transduction pathways. Indeed, Schreck *et al.*[8,56] have shown that NF-κB activation in Jurkat T cells can be partly counteracted by deferoxamine and *O*-phenanthroline. This inhibition is likely to act at an early stage, i.e., in the generation of highly oxidative radicalar oxygen species from H_2O_2. After TNF-α stimulation, DFO protects against HIV-1 activation in the absence of a clear effect on NF-κB. In this case, iron chelation probably acts primarily by targeting cellular ribonucleotide reductase, as discussed above.

The present report is mainly based on the study of two cell lines, often used for studying the mechanisms of HIV-1 gene transcription and virus activation. Although this study has also been extended to PMBC in primary culture, the results obtained with iron chelators in these *in vitro* systems do, therefore, not allow any present extrapolation on the possible clinical usefulness of these compounds in HIV infected patients. However, they indicate that iron plays an important role in triggering the generation of oxidative stress, with the deleterious consequences on activation of NF-κB and on subsequent activation of HIV-1 transcription. This may be of relevance, as iron is known to accumulate, in patients with AIDS, in several types of cells, such as macrophages and microglia.[57,58] Iron loading in certain tissues may be deleterious, not only by increasing oxidative stress and directly activating HIV, but also by decreasing immunological defenses and by providing iron as nutrient for the growth of several microbial invaders.[59]

The three previously reported *in vitro* studies on a possible antiretroviral effect of DFO have reached contradictory results.[60–62] Tabor *et al.*[60] reported that 30 μM DFO inhibited the expression of p24 antigen in infected H9 lymphocyte, and Baruchel *et al.*[61] found that 18 μM DFO reduced reverse transcriptase activity in infected MT4 cells, but had a less marked effect on p24 antigen expression. Finally, Lazdins *et al.*[62] re-

RNSDOCID: <XP___2104894A__1_>

ported that DFO has no anti-HIV effects *in vitro*, either in H9 cells or in three other cell lines surveyed. It is thus difficult to draw firm conclusions from these contradictory findings. It is important to realize that none of these three brief reports mentioned any study on the effects of DFO on HIV-infected cells submitted to an oxidative stress. By contrast, the present study examined the effect of iron chelators in such cells, activated by an oxidative stress, which may be more relevant to the clinical situation.[4–6,14,15] In this setting, iron chelation by either DFO or several chemically unrelated compounds clearly affords a protection against cytotoxicity and it results in antiretroviral activity *in vitro*. We suggest that iron chelation therapy may become a new tool, helping to slow the progression of HIV infection. It should be noted that the concentration range at which several iron chelators were found *in vitro* to inhibit oxidative stress-induced activation of NF-κB and of HIV (e.g., DFO at 5 μM and L1 at 60 μM) is easily achieved in humans.[63,64] Furthermore, a retrospective study has recently been reported that investigated the course of HIV infection in 64 seropositive patients with thalassemia major who were treated by DFO.[65] The outcome of HIV infection was significantly better in the patient group treated with more than 40 mg/kg per day of DFO than in the group treated with a lower DFO dose.[65] Although this favorable result is in keeping with the conclusions from the present experiments, careful prospective clinical studies are obviously needed to assess a possible benefit of iron chelation therapy to HIV-infected patients.

ACKNOWLEDGMENTS

This work was supported by a grant from the Belgian National Fund for Scientific Research (Brussels, Belgium) and by the Belgian National Lottery. C.S. is supported by a fellowship from the *Communauté Française de Belgique*. S.L-P. by a grant from the Belgian National Fund for Scientific Research (Brussels, Belgium), and J.P. is Research Director of the Belgian National Fund for Scientific Research (Brussels, Belgium). The authors wish to express their gratitude to all those who kindly provided the experimental iron chelators, in particular Prof. A. Shanzer and Dr. R.W. Grady. They also thank the NIH AIDS Research and Reference Reagent Program for providing U1 and ACH-2 cell lines, and Douglas Craig for careful reading of the manuscript.

REFERENCES

1. Fauci AS: Multifactorial nature of human immunodeficiency virus disease: Implication for therapy. Science 1993;262:1011–1018.
2. Pantaleo G and Fauci A: Tracking HIV during disease progression. Curr Opin Immunol 1994;6:600–604.
3. Ho W-Z and Douglas SD: Glutathione and *N*-acetylcysteine suppression of HIV replication in human monocytes/macrophages *in vitro*. AIDS Res Hum Retroviruses 1992;8:1249–1253.
4. Staal FJT, Ela SW, Roederer M, Anderson MT, Herzenberg LA, and Herzenberg LA: Glutathione deficiency and human immunodeficiency virus infection. Lancet 1992;339:909–912.
5. Eck H-P, Gmunder H, Hartmann M, Petzoldt D, Daniel V, and Droge W: Low concentrations of acid-soluble thiol (cysteine) in the blood of HIV-1 infected patients. Biol Chem Hoppe-Seyler 1989;370:101–107.
6. Buhl R, Holroyd KJ, Mastrangeli A, Cantin AM, Jaffe HA, Wells FB, Saltini C, and Crystal RG: Systemic glutathione deficiency in symptom free HIV-seropositive individuals. Lancet 1989;2:1294–1296.
7. Legrand-Poels S, Vaira D, Pincemail J, Van de Vorst A, and Piette J: Activation of human immunodeficiency virus type 1 by oxidative stress. AIDS Res Hum Retroviruses 1990;6:1389–1397.
8. Schreck R, Rieber P, and Baeuerle PA: Reactive oxygen intermediates as apparently widely used messengers in the activation of NF-κB transcription factor and HIV-1. EMBO J 1991;10:2247–2258.
9. Roederer M, Staal FJT, Raju PA, Ela SW, Herzenberg LA, and Herzenberg LA: Cytokine-stimulated HIV replication is inhibited by *N*-acetyl-L-cysteine. Proc Natl Acad Sci USA 1990;87:4884–4888.
10. Kabelic T, Kinter A, Poli G, Anderson ME, Meister A, and Fauci AS: Suppression of human immunodeficiency virus expression in chronically infected monocyte cells by glutathione, glutathione ester, and *N*-acetylcysteine. Proc Natl Acad Sci USA 1991;88:986–990.
11. Sappey C, Legrand-Poels S, Best-Belpomme M, Favier A, Rentier B, and Piette J: Stimulation of glutathione peroxidase activity decreases HIV-1 activation after oxidative stress. AIDS Res Hum Retroviruses 1994;10:1447–1457
12. Roederer M, Staal FJT, Osada H, Herzenberg L, and Herzenberg L: CD4 and CD8 T cells with high intracellular glutathione levels are selectively lost as the HIV infection progresses. Int Immunol 1991;3:933.
13. Staal FJT, Anderson MT, Staal GE, Herzenberg LA, Gitler C, and Herzenberg LA: Redox regulation of signal transduction: Tyrosine phosphorylation and calcium influx. Proc Natl Acad Sci USA 1994;91:3619–3622.
14. Buhl R: Imbalance between oxidants and antioxidants in the lungs of HIV seropositive individuals. Chem-Biol Interact 1994;91:147–158.
15. Staal FJT, Roederer M, Israelski DM, Bubp J, Mole LA, McShane D, Derenzinski SC, Russ W, Sussman II, Raju PA, Anderson MT, Moore W, Ela SW, Herzenberg LA, and Herzenberg LA: Intracellular glutathione levels in T cell subsets decrease in HIV infected individuals. AIDS Res Hum Retroviruses 1992;8:305–311.
16. Sandstrom PA, Roberts B, Folks TM, and Buttke TM: HIV gene expression enhances T cell susceptibility to hydrogen peroxide-induced apoptosis. AIDS Res Hum Retroviruses 1993;9:1107–1113.
17. Haseltine W: *Control of Human Retrovirus Gene Expression*. Cold Spring Harbor Laboratory, Cold Spring Harbor, NY, 1988.
18. Nabel G and Baltimore D: An inducible transcription factor activates expression of human immunodeficiency virus in T cells. Nature (London) 1987;326:711–713.
19. Baeuerle PA and Baltimore D: IκB: A specific inhibitor of the NF-κB transcription factor. Science 1988;242:540–546.
20. Ghosh S and Baldmore D: Activation *in vitro* of NF-κB by phosphorylation of its inhibitor IκB. Nature 1990;344:678–682.
21. Horvat RT and Wood CJ: Promotor activity in primary antigen-specific human T lymphocytes. J Immunol 1989;132:2745–2751.
22. Hazan U, Thomas D, Alcami J, Bachelerie F, Israel N, Yssel Y, Virelizier JL, and Arenzana-Seisdedos F: Stimulation of a human T-cell clone with an anti-CD3 or tumor necrosis factor induces NF-κB translocation but not human immunodeficiency virus-1 enhancer-dependent transcription. Proc Natl Acad Sci USA 1990;87:7861–7865.
23. Folks TM, Justement J, Kinter A, Schnittman S, Orenstein J, Poli G, and Fauci AS: Characterization of a promonocyte clone chron-

12. Juli 2004 14:57 Lee & Stiefel Nr. 0819 P. 15

ically infected with HTV-1 and inducible by 13-phorbol-12-myristate acetate. J Immunol 1988;140:1117–1122.
24. Clouse KA, Powell D, Washington I, Poli G, Strebel K, Farrar W, Barstad P, Kovacs J, Fauci AS, and Folks TM: Monokine regulation of human immunodeficiency virus-1 expression in a chronically infected human T cell clone. J Immunol 1989;142:431–438.
25. Halliwell B: Free radicals, antioxidants, and human disease: Curiosity, cause, or consequence? Lancet 1994;344:721–724.
26. Flohe L: Glutathione-peroxidase brought into focus. In: *Free Radicals in Biology*. Pryor WA (Ed). Academic Press, New York, 1982, pp. 223–254.
27. Haber F and Weiss J: The catalytic decomposition of hydrogen peroxide by iron salts. Proc Roy Soc London A 1934;147:332–351.
28. Minotti G and Aust SD: The role of iron in oxygen radical mediated lipid peroxidation. Chem-Biol Interact 1989;71:1–19.
29. Sies H: Biochemistry of oxidative stress. Angew Chem Int Ed Engl 1986;25:1058–1071.
30. Japour AJ, Mayers DL, Johnson VA, Kuritzer DR, Becker LA, Arduino JM, Lane J, Black RJ, Reichelderfer PS, d'Aquila RT, Crumpacker CS, and the RV-43 study group and the AIDS clinical trials group virology committee resistance working group: Standardized peripheral blood mononuclear cell culture assay for the determination of drug susceptibilities of clinical human immunodeficiency type 1 isolates. Antimicrob Agent Chemother 1993;37:1095–1101.
31. Grady RW and Jacobs A: The screening of potential iron chelating drugs. In: *Development of Iron Chelators for Clinical Use*. Martell AE, Anderson W-F, and Badman DG (Eds). Elsevier/North-Holland, Amsterdam, 1981, p. 133.
32. Brittenham GM: Development of iron-chelating agents for clinical use. Blood 1992;80:569–574.
33. Shanzer A, Libman J, Lytton SD, Glickstein H, and Cabantchik ZI: Reversed siderophores act as antimalarial agents. Proc Natl Acad Sci USA 1991;88:6585–6589.
34. Hoffman AD, Banapour B, and Levy JA: Characterization of the AIDS-associated retrovirus reverse transcriptase and optimal conditions for its detection in virions. Virology 1985;147:326–335.
35. Andrews NC and Faller DV: A rapid micropreparation technique for extraction of DNA binding proteins from limiting numbers of mammalian cells. Nucleic Acids Res 1991;19:2499.
36. Dignam D, Lebovitz RM, and Roeder RG: Accurate transcription initiation by RNA polymerase II in a soluble extract from isolated mammalian nuclei. Nucleic Acids Res 1983;11:1475–1489.
37. Meyer M, Schreck R, and Baeuerle PA: H_2O_2 and antioxidants have opposite effects on activation of NF-κB and AP-1 in intact cells: AP-1 as secondary antioxidant responsive factor. EMBO J 1993;12:2005–2015.
38. Hoffbrand AV, Ganeshaguru K, Hooton JWL, and Tattersall MHN: Effect of iron deficiency and desferrioxamine on DNA synthesis in human cells. Br J Haematol 1976;33:517–521.
39. Marx JL: Oxygen free radicals linked to many diseases. Science 1987;235:529–531.
40. Raju PA, Herzenberg LA, Herzenberg LA, and Roederer M: Glutathione precursor and antioxidant activities of N-acetylcysteine and oxothiazolidine carboxylate compared in *in vitro* studies of HIV replication. AIDS Res Hum Retroviruses 1994;10:961–967.
41. Kemp JD: The role of iron and iron binding proteins in lymphocyte physiology and pathology. J Clin Immunol 1993;13:81–92.
42. Bonfort A, Young SP, Nouri-Arai K, and William R: Uptake and release of transferrin and iron by mitogen-stimulated human lymphocytes. Br J Haematol 1983;55:93–101.
43. Parthasarathy K, Hoy TG, and Jacobs A: Effect of phytohaemagglutinin on the synthesis and secretion of ferritin in peripheral blood lymphocytes. Br J Haematol 1988;69:567–570.
44. Wrigglesworth JM and Baum H: *Iron in Biochemistry and Medicine II*. Jacobs A and Worwood M (Eds). Academic Press, New York, 1980, pp. 22–47.
45. Ford GC, Harrison PM, Rice DW, Smith JMA, Treffry A, White JL, and Yariv J: Ferritin: Design and function of an iron-storage molecule. Phil Trans R Soc London 1984;B304:551–565.
46. Chasteen ND: The identification of the probable locus of iron and anion binding in the transferrins. Trends Biochem Sci 1983;8:272–275.
47. Gutteridge JM, Richmond R, and Halliwell B: Inhibition of the iron-catalysed formation of hydroxyl radicals from superoxide and of lipid peroxidation by desferrioxamine. Biochem J 1979;184:469–472.
48. Voest EE, Vreugdenhil G, and Marx JJM: Iron-chelating agents in non-iron overload conditions. Ann Intern Med 1994;120:490–499.
49. Lederman HM, Cohen A, Lee JWW, Freidman MH, and Gelfand EW: Desferrioxamine: A reversible S-phase inhibitor of human lymphocyte proliferation. Blood 1984;64:748–753.
50. Porter JB: Oral iron chelators: Prospects for future development. Eur J Haematol 1989;43:271.
51. Malley SD, Grange JM, Hamedi-Sangsari F, and Vila JR: Synergistic anti-human immunodeficiency virus type 1 effect of hydroxamate compounds with 2',3'-dideoxyinosine in infected resting human lymphocytes. Proc Natl Acad Sci USA 1994;91:11017–11021.
52. Halliwell B and Gutteridge JMC: In: *Free Radicals in Biology and Medicine*. Clarendon Press, Oxford, 1989, pp. 22–47.
53. Schieven GL, Kirihara JM, Burg DL, Geahlen RL, and Ledbetter JA: $p72^{syk}$ tyrosine kinase is activated by oxidizing conditions that induce lymphocyte tyrosine phosphorylation and Ca^{2+} signals. J Biol Chem 1993;268:16688–16692.
54. Schieven GL, Kirihara JM, Myers DE, Ledbetter JA, and Uckun FM: Reactive oxygen intermediates activate NF-κB in a tyrosine kinase-dependent mechanism and in combination with vanadate activate the $p56^{lck}$ and $p59^{fyn}$ tyrosine kinases in human lymphocytes. Blood 1993;82:1212–1220.
55. Schieven GL, Mittler RS, Nadler SG, Kirihara JM, Bolen JB, Kanner SB, and Ledbetter JA: ZAP-70 tyrosine kinase, CD45, and T cell receptor involvement in UV- and H_2O_2-induced T cell signal transduction. J Biol Chem 1994;269:20718–20726.
56. Schreck R, Meier B, Mannel DM, Droge W, and Baeuerle PA: Dithiocarbamates as potent inhibitors of nuclear factor kappa B activation in intact cells. J Exp Med 1992;175:1181–1194.
57. Diebold J, Tabbara W, Marche C, Audouin J, and Le Tourneau A: Modifications de la moelle osseuse à divers stades de l'infection par VIH étudiées par biopsie médullaire chez 85 patients. Arch Anat Cytol Pathol 1991;39:137–146.
58. Gelman BB, Rodriguez-Wolf MG, Wen J, Kumar S, Campbell GR, and Herzog N: Siderotic cerebral macrophages in the acquired immunodeficiency syndrome. Arch Pathol Lab Med 1992;116:509–516.
59. Weinberg ED: Iron and infection. Microbiol Rev 1978;42:45–66.
60. Tabor E, Epstein JS, Howley IK, and Lee SF: Inhibition by desferrioxamine of *in vitro* replication of HIV-1. Lancet 1991;337:795.
61. Baruchel S, Gao Q, and Wainberg MA: Desferrioxamine and HIV. Lancet 1991;337:1356.
62. Lazdins JK, Alteri E, Klimkait T, Woods-Cook K, Walker MR, Gaarte G, and Poncioni B: Lack of effect of desferrioxamine on *in vitro* HIV-1 replication. Lancet 1991;338:1341.
63. Matsui D, Klein J, Hermann C, Grunau V, McClelland R, Chung D, St-Louis P, Olivieri N, and Koren G: Relationship between the pharmacokinetics and iron excretion pharmacodynamics of the new iron chelator 1,2 dimethyl-3-hydroxypyrid-4-one in patients with thalassemia. Clin Pharmacol Ther 1991;50:294–298.
64. Verpooten GA, D'Haese PC, Boelaert JR, Bocaus I, Lamberts LV,

BNSDOCID: <XP 2104523A 1 >

and De Broe ME: Pharmacokinetics of aluminoxamine and ferrioxamine and dose finding of desferrioxamine in haemodialysis patients. Nephrol Dial Transplant 1992;7:931–938.
65. Costiaglioga D, de Montalembert M, Lefèvre J-J, Briand C, Rebulla P, Baruchel S, Dessi C, Fondu P, Karagiorga M, Perrimond H, and Girod R: Dose of desferrioxamine and evolution of HIV-1 infection in thalassaemic patients. Br J Haematol 1994;87:549–552

Address reprint requests to:
Jacques Piette
Laboratory of Virology
Institute of Pathology B23
University of Liège
B-4000 Liège, Belgium

SNSDOCID: <XP___2104523A_1_>

****
*** ACTIVITY REPORT ***
****

RECEPTION OK

TX/RX NO.	9908
CONNECTION TEL	+31 20 6260007
CONNECTION ID	
START TIME	07/12 06:44
USAGE TIME	10'07
PAGES	16
RESULT	OK

Am J Physiol Lung Cell Mol Physiol 282: L1349–L1357, 2002.
First published January 18, 2002; 10.1152/ajplung.00338.2001.

Bleomycin upregulates expression of γ-glutamylcysteine synthetase in pulmonary artery endothelial cells

REGINA M. DAY,[1] YUICHIRO J. SUZUKI,[2] JULIE M. LUM,[1]
ALEXANDER C. WHITE,[1] AND BARRY L. FANBURG[1]
[1]*Pulmonary and Critical Care Division, Tupper Research Institute, New England Medical Center; and* [2]*Jean Mayer United States Department of Agriculture Human Nutrition Research Center on Aging at Tufts University, Boston, Massachusetts 02111*

Received 27 August 2001; accepted in final form 9 January 2002

Day, Regina M., Yuichiro J. Suzuki, Julie M. Lum, Alexander C. White, and Barry L. Fanburg. Bleomycin upregulates expression of γ-glutamylcysteine synthetase in pulmonary artery endothelial cells. *Am J Physiol Lung Cell Mol Physiol* 282: L1349–L1357, 2002. First published January 18, 2002; 10.1152/ajplung.00338.2001.—The chemotherapeutic agent bleomycin induces pulmonary fibrosis through the generation of reactive oxygen species (ROS), which are thought to contribute to cellular damage and pulmonary injury. We hypothesized that bleomycin activates oxidative stress response pathways and regulates cellular glutathione (GSH). Bovine pulmonary artery endothelial cells exposed to bleomycin exhibit growth arrest and increased cellular GSH content. γ-Glutamylcysteine synthetase (γ-GCS) controls the key regulatory step in GSH synthesis, and Northern blots indicate that the γ-GCS catalytic subunit [γ-GCS heavy chain (γ-GCS_h)] is upregulated by bleomycin within 3 h. The promoter for human γ-GCS_h contains consensus sites for nuclear factor-κB (NF-κB) and the antioxidant response element (ARE), both of which are activated in response to oxidative stress. Electrophoretic mobility shift assays show that bleomycin activates the transcription factor NF-κB as well as the ARE-binding factors Nrf-1 and -2. Nrf-1 and -2 activation by bleomycin is inhibited by the ROS quenching agent *N*-acetylcysteine (NAC), but not by U-0126, a MEK1/2 inhibitor that blocks bleomycin-induced MAPK activation. In contrast, NF-κB activation by bleomycin is inhibited by U-0126, but not by NAC. NAC and U-0126 both inhibit bleomycin-induced upregulation of γ-GCS expression. These data suggest that bleomycin can activate oxidative stress response pathways and upregulate cellular GSH.

reactive oxygen species; Nrf-1 and -2; nuclear factor-κB; antioxidant response element; mitogen-activated protein kinase

BLEOMYCIN IS PRIMARILY USED for the treatment of testicular carcinoma, lymphoma, and squamous cell carcinoma, but its use as a chemotherapeutic agent is limited by adverse side effects, especially pulmonary injury and fibrosis. Because of this, bleomycin has been used to develop a rodent experimental model of pulmonary fibrosis that has allowed the study of changes in the cellular composition of the lung and the expression of specific proteins leading to fibrosis. Many changes identified in the bleomycin model system have also been observed in pulmonary fibrosis induced by other causes (2, 20, 21, 30). Treatment of rodents with bleomycin endotracheal instillation or subcutaneous injection results in initial pulmonary inflammation and a spike of epithelial/endothelial apoptosis (13, 30, 38, 46). This is followed by the proliferation of myofibroblasts (fibroblasts expressing α-smooth muscle actin) and sustained epithelial/endothelial apoptosis. The bleomycin model has allowed the identification of potentially critical changes in protein expression, including the induction of transforming growth factor-β1 (18, 26, 27, 29, 30). However, the signaling mechanism(s) inducing these changes is not well understood.

Bleomycin triggers apoptosis in growing cells by causing single- and double-stranded DNA breaks through the direct binding of bleomycin to DNA. This activity is dependent on oxygen and a bound ferrous ion. Bleomycin is also believed to produce reactive oxidative species (ROS), including superoxide, H_2O_2, and/or organoperoxides, which may also play a role in the toxicity of bleomycin (34). Several studies have shown that cells are partially protected from the cytotoxic effects of bleomycin by acute hypoxia (thus eliminating the oxygen source for ROS) or by the addition of superoxide dismutase enzyme or transfection with an expression vector for superoxide dismutase (thus reducing the level of ROS generated by bleomycin) (10, 34). In contrast, the detrimental effects of bleomycin can be intensified via reduction of the intrinsic cellular defenses against oxidative stress. Either buthionine sulfoximine (BSO)-induced depletion of cellular glutathione (GSH) or the lack of GSH *S*-transferase (a phase II detoxifying enzyme) results in hypersensitivity of cells to bleomycin-induced apoptosis (12, 31).

On the basis of studies indicating that bleomycin cytotoxicity may be modulated by oxidants and antioxidants, we hypothesized that bleomycin may regulate cellular defenses against oxidative stress. GSH is a

Address for reprint requests and other correspondence: R. M. Day, New England Medical Center, Pulmonary and Critical Care Division, NEMC #257, 750 Washington St., Boston, MA 02111 (E-mail: rday@lifespan.org).

The costs of publication of this article were defrayed in part by the payment of page charges. The article must therefore be hereby marked "*advertisement*" in accordance with 18 U.S.C. Section 1734 solely to indicate this fact.

ubiquitous sulfhydryl-containing tripeptide that serves as a primary biological defense against oxidative damage (6, 33, 37, 44). GSH, normally present in cells at millimolar levels, directly interacts with ROS and toxins during cellular detoxification (6, 37, 44). Adaptation of cells to oxidative stress can occur via the induction of antioxidant enzymes and increased cellular levels of GSH. The enzyme γ-glutamylcytsteine synthetase (γ-GCS) controls the rate-limiting step in GSH synthesis (16, 17, 24). This enzyme is composed of two subunits, a catalytic heavy chain (γ-GCS_h) and a regulatory light chain. Both γ-GCS subunits have been shown to be upregulated in response to oxidative stress, including ionizing radiation, ROS, heavy metals, phenolic antioxidants, and the GSH-depleting compound BSO (16, 17, 32, 33, 36, 41, 44). The regulation of the γ-GCS subunits by oxidative stress has been demonstrated in variety of species, including human, rat, and bovine (32, 33, 36, 44).

In the present study, we examined the effect of bleomycin on the regulation of GSH in bovine pulmonary artery endothelial cells (BPAEC). Our results indicate that bleomycin treatment increases total cellular levels of GSH and upregulates the level of γ-GCS_h mRNA. We also show that bleomycin activates the DNA binding activity of nuclear factor (NF)-κB and Nrf-1 and -2 transcription factors. These factors are known to be activated by oxidative stress and to regulate the expression of human γ-GCS_h (14–17, 24, 40, 41, 44, 45).

EXPERIMENTAL METHODS

Reagents. Bleomycin (Blenoxane) was from Mead Johnson (Princeton, NJ). The mitogen-activated protein kinase/extracellular signal-regulated kinase [MAPK/ERK (MEK)] 1/2 inhibitor U-0126 was purchased from New England Biolabs (Beverly, MA). Other reagents are described below.

Cell culture and bleomycin treatment. BPAEC were obtained from freshly slaughtered calves as previously described (4). *Passage 3–8* cells were used for all experiments. Rat pulmonary microvascular endothelial cells (RPMEC) were a gift of Dr. Una Ryan (Avant Immunotherapeutics, Needham, MA) (3); these cells were used as a control in Fig. 2. Both BPAEC and RPMEC were cultured in RPMI 1640 (GIBCO-BRL, Rockville, MD) with antibiotics (penicillin and streptomycin), fungisone, and 10% fetal bovine serum in 5% CO_2 at 37°C in a humidified atmosphere. For cell culture treatment, bleomycin was dissolved in 0.9% NaCl and added to the culture medium.

Propidium iodide staining and fluorescence activated cell sorting. Propidium iodide and fluorescence-activated cell sorting (FACS) were used to determine cellular apoptosis. Cells (~3–7.5 × 10^5) were washed twice with phosphate-buffered saline (PBS) at 25°C and trypsinized. Cells were then pelleted by centrifugation and washed twice on ice with cold PBS. After the last wash, we resuspended cell pellets in 100 μl of cold PBS, and added 1 ml of cold 80% ethanol dropwise while vortexing on a low setting. Ethanol-treated cells were stored at 4°C for at least 4 h and up to 1 wk. Before FACS analysis, cells were pelleted at 4°C, resuspended in 0.5 ml of propidium iodide solution [0.05 mg/ml RNase A in PBS containing 5% (wt/vol) propidium iodide], and incubated for 30 min on ice in the dark. Cells were then analyzed on a Becton-Dickinson FACS Calibur (Franklin Lakes, NJ) cell sorter.

Cell counts and preparation for GSH assays. Cell counts and GSH assays were performed as described (43). Culture dishes were rinsed twice with PBS at 25°C and incubated for 3–5 min with 1.0 ml of trypsin-EDTA. The cells were rapidly suspended and placed on ice. The cellular suspension (0.1 ml) was removed, diluted, and counted on a ZM Coulter Counter (Coulter Electronics, Hialeah, FL). Of the remaining suspension, 0.8 ml was treated with 0.1 ml of 1% perchloric acid. Lysates were sonicated on ice for 10 s and centrifuged at 14,000 *g* at 4°C for 20 min. Aliquots were stored at −20°C for GSH assays.

GSH assay. GSH assays were performed as specified (40). Frozen perchloric acid-treated supernatants were thawed on ice and sonicated for 10 s on ice. The pH was adjusted to 7.0 with 0.3 M potassium hydroxide-3-(*N*-morpholino)propanesulfonic acid (MOPS). The sonicate was then centrifuged at 14,000 *g* at 4°C for 20 min. The supernatant was assayed for total cellular GSH by the spectrophotometric Tietze method (1). Briefly, the sum of the oxidized and reduced forms of GSH was determined using a kinetic assay in which GSH or GSH disulfide and GSH reductase reduce 5,5′-dithiobis(2-nitrobenzoic acid) to form 5-thio-2-nitrobenzoate (TNB). The formation of TNB was followed spectrophotometrically at 412 nm. Each assay was individually calibrated with standard GSH, and the concentration of each sample was adjusted by dilution to ensure that the reaction rate was on the linear portion of the standard curve. Cellular GSH levels were expressed as nanomoles per 10^6 cells. For the assay, brewer's yeast GSH reductase, β-NADPH, and GSH disulfide were obtained from Sigma (St. Louis, MO).

RNA purification and Northern blot. RNA was purified using Trizol (GIBCO-BRL) according to the manufacturer's instructions; RNA concentrations were determined by absorbance at 260 nm. RNA (10 μg) was denatured in a loading buffer [0.4 M MOPS, pH 7.0, 2.5% formaldehyde, 67% formamide, 0.2 μg ethidium bromide, 1.2 mM EDTA, 6.7 mM Na acetate, and 13% dye (50% glycerol, 1 mM EDTA, 0.25% bromophenol blue, and 0.25% xylene cyanol FF)] for 15 min at 65°C. Denatured RNA was run in a 0.9% (wt/vol) denaturing agarose gel (0.2 M MOPS, pH 7.0, 5 mM sodium acetate, 1 mM EDTA, and 1.8% formaldehyde) with running buffer (0.2 M MOPS, pH 7.0, 5 mM Na acetate, 1 mM EDTA, and 1.8% formaldehyde). RNA was transferred to a Zeta Probe blotting membrane (Bio-Rad, Hercules, CA) using capillary blotting in 1× SSC (20× SSC = 3 M NaCl, 3 mM sodium citrate, pH 7.0). Blots were baked at 80°C for 2 h under vacuum and prehybridized in ExpressHyb (Clontech, Palo Alto, CA) for 30 min at 68°C under shaking. The 2 × 10^6 counts·min^{-1}·ml^{-1} of labeled, denatured probe were then added with denatured salmon sperm DNA (100 ng/ml) to the prehybridized blot. Hybridization was performed at 68°C overnight with agitation. Blots were washed at 37°C; the first wash was performed in triplicate (2× SSC and 0.05% SDS) for 15 min each; the second wash was done twice (1× SSC and 0.1% SDS) for 15 min each at 50°C. The blot was then exposed to Kodak X-OMAT AR film (NEN, Boston, MA) at −80°C using intensifying screens.

The probe for human γ-GCS_h was the gift of Dr. Takahito Kondo (Nagasaki University School of Medicine, Nagasaki, Japan); this probe hybridizes strongly to human, mouse, and rat γ-GCS_h mRNA (16). To produce labeled probes, we incubated 10–20 ng of the excised γ-GCS_h cDNA with 1× hexanucleotide mix (Boehringer Mannheim, Indianapolis, IN), 0.05 mM dATP, dTTP, and dGTP, and 50 μCi α-[^{32}P]dCTP for 1 h at 37°C. The labeled probe was purified from unincor-

porated α-[^{32}P]dCTP using Sephadex G-50 Quick Spin columns (Boehringer Mannheim).

Electrophoretic mobility shift assay. Electrophoretic mobility shift assay (EMSA) was performed as described by Garner and Revzin (11). To prepare nuclear extracts, cells were washed in PBS and incubated in 10 mM HEPES (pH 7.8), 10 mM KCl, 2 mM $MgCl_2$, 0.1 mM EDTA, 0.1 mM phenylmethylsulfonyl fluoride (PMSF), 5 μg/ml leupeptin, 10 μg/ml aprotinin, 1 mM NaF, 0.1 mM sodium orthovanadate, and 1 mM tetrasodium pyrophosphate for 15 min at 4°C. (Octylphenoxy)polyethoxyethanol (Igepal CA-630, Sigma) was then added at a final concentration of 0.6%(vol/vol). Samples were vortexed and centrifuged. Pelleted nuclei were resuspended in extraction buffer [50 mM HEPES (pH 7.8), 50 mM KCl, 300 mM NaCl, 0.1 mM EDTA, 0.1 mM PMSF, 5 μg/ml leupeptin, 10 μg/ml aprotinin, 1 mM NaF, 0.1 mM sodium orthovanadate, 1 mM tetrasodium pyrophosphate, and 1% (vol/vol) glycerol], then mixed vigorously for 20 min, and centrifuged for 5 min. The supernatants were harvested, and protein concentrations were determined (22).

Oligonucleotides containing the sense and antisense antioxidant response element (ARE) consensus sequence were 5′-TCACAGTGACTCAGCAGAATC-3′ and 5′-GATTCTGCTGAGTCA-CTGTGA-3′, respectively. [The ARE consensus sequence is underlined; the ARE sequence used is identical to ARE4 of the human γ-GCS promoter (25, 42).] Oligos were made 5 μM in H_2O, heated to 80°C for 20 min, and allowed to anneal by cooling slowly to ambient temperature. The double-stranded oligonucleotide probe containing consensus κB sequence was 5′-GAT CCG AGG GGA CTT TCC GCT GGG GAC TTT CCA GG-3′. To perform EMSA, we incubated binding reaction mixtures containing 2 μg protein of nuclear extract, 1 μg poly(dI-dC)·poly(dI-dC), and ^{32}P-labeled double-stranded ARE or κB oligonucleotide in 100 mM NaCl, 1 mM EDTA, 1 mM dithiothreitol, 10% (vol/vol) glycerol, and 20 mM Tris·HCl (pH 7.5) for 20 min at 25°C. Electrophoresis of samples through a native 6% polyacrylamide gel (acrylamide-bis, 29:1) was followed by autoradiography. Supershift experiments were performed by incubating 2 μg Nrf-1, Nrf-2, c-Jun, c-Fos, NF-κB p65, or NF-κB p50 antibody (Santa Cruz Biotech) in the binding reaction mixture for 1 h at 4°C before the addition of the ^{32}P-labeled oligonucleotide probe to start the binding reaction. All experiments were repeated at least three times.

Western blot analysis. To prepare lysates, cells were washed in PBS and solubilized with 50 mM HEPES solution (pH 7.4) containing 1% (vol/vol) Triton X-100, 4 mM EDTA, 1 mM NaF, 0.1 mM sodium orthovanadate, 1 mM tetrasodium pyrophosphate, 2 mM PMSF, 10 μg/ml leupeptin, and 10 μg/ml aprotinin. The lysate was cleared by centrifugation at 4°C for 15 min. Protein concentrations in the supernatant were determined as above (22). Cell lysates (10 μg protein) were electrophoresed through reducing (5% β-mercaptoethanol) SDS polyacrylamide-bis gels (10%) and electroblotted onto nitrocellulose membranes. After the transfer, membranes were blocked in 5% milk in Tween- and Tris-buffered saline (20 mM Tris·HCl, pH 7.5, 150 mM NaCl, and 0.05% Tween 20) and then blotted with the antibody for the NF-κB p65 subunit and IκBα (Santa Cruz Biotech). Levels of proteins and phosphoproteins were detected with horseradish peroxidase-linked secondary antibodies and ECL System (Amersham Life Science, Arlington Heights, IL). Western blots were repeated at least three times.

Statistics. Statistical comparisons were performed using a Student's *t*-test for unpaired samples and a two-way analysis of variance for multiple comparisons. Statistical significance was determined at $P < 0.05$.

RESULTS

Bleomycin upregulates cellular GSH and the γ-GCS gene. Bleomycin has been shown to induce growth arrest, apoptosis, and necrosis in a number of cells, including immortalized cells and primary cancer cells (31, 34). We first determined doses of bleomycin that induce growth arrest with limited cell death in BPAEC. Cells were placed in RPMI medium containing 0.1% FBS for 24 h and then exposed to increasing doses of bleomycin for 24 h. Cell numbers indicated that 10 μg/ml of bleomycin induced high levels of growth arrest (Fig. 1*A*), which was associated with visible cell death (data not shown). Levels of 1.0 and 0.1 μg/ml of bleomycin induced lower levels of growth arrest. Propidium iodide staining and FACS analysis showed that 1.0 μg/ml of bleomycin induced only 8.8% (± 1.6 SD) apoptosis, compared with 5.8% (± 1.7 SD) apoptosis in control cells ($n = 3$).

Bleomycin is believed to induce oxidative stress on cells by the generation of ROS through a bound ferrous ion. GSH is a primary constituent for protecting cells against oxidative stress, and its formation can be upregulated by ROS-producing compounds (6, 32, 33, 44).

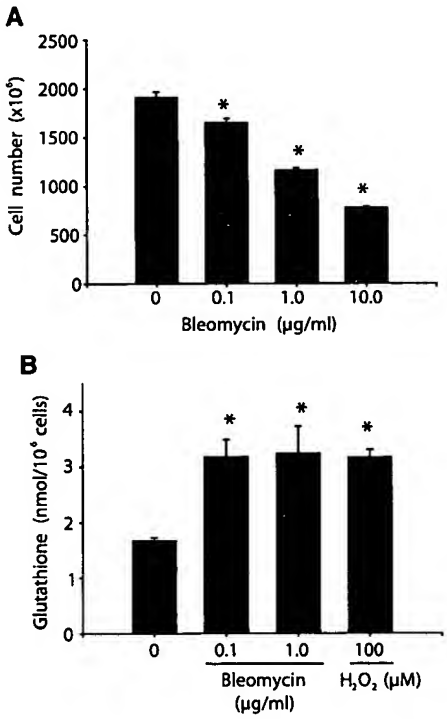

Fig. 1. Bleomycin causes growth arrest in bovine pulmonary artery endothelial cells (BPAEC) and upregulates cellular levels of glutathione (GSH). *A*: BPAEC were plated at 4 × 10^4 cells/35 mm dish for 48 h before being placed in RPMI-0.1% fetal bovine serum (FBS) for 24 h and then exposed for 24 h to the presence or absence of bleomycin before counting. Under these conditions, BPAEC continue to grow slowly for up to 72 h in the absence of serum. Values represent means ± SE, $n = 5$. *Significantly different from the control value without bleomycin treatment. *B*: BPAEC were plated at 4 × 10^4 cells/35-mm dish for 48 h before being placed in RPMI-0.1% FBS for 24 h and then exposed to bleomycin or H_2O_2. Total GSH levels were measured after 18 h of treatment. Values represent means ± SE, $n = 4$. *Significantly different from the control.

We analyzed total cellular GSH to determine whether bleomycin was able to regulate GSH formation. A spectrophotometric assay for total cellular GSH showed that both 0.1 and 1.0 μg/ml of bleomycin caused approximately twofold increases within 18 h compared with control (Fig. 1*B*). These results were comparable with the twofold increase in total cellular GSH induced by an 18-h treatment with 100 μM H_2O_2, used as a positive control (43).

The enzyme γ-GCS controls the key regulatory step in the production of cellular GSH (6, 35, 44). Northern blot analysis shows that γ-GCS_h mRNA levels are upregulated by bleomycin in BPAEC. Figure 2*A* is a representative time course in which γ-GCS_h mRNA is increased by 30 min in response to 1 μg/ml of bleomycin. BSO, an agent known to induce γ-GCS_h expression, was used as a positive control (44). Our probe for γ-GCS_h is based on rat cDNA, but the bovine size, sequence, and, therefore, complementarity to rat γ-GCS_h are not known. The rat mRNA was included as a positive control for the position of γ-GCS_h (Fig. 2*A*). Densitometry of the representative data showed that within 30 min, bleomycin caused a 1.5-fold increase in γ-GCS_h mRNA levels, whereas at 3–6 h bleomycin induced a 3–3.5-fold increase (Fig. 2*C*). BSO exposure for 3 and 6 h induced a 2.5- and 2-fold increase in γ-GCS_h mRNA, respectively.

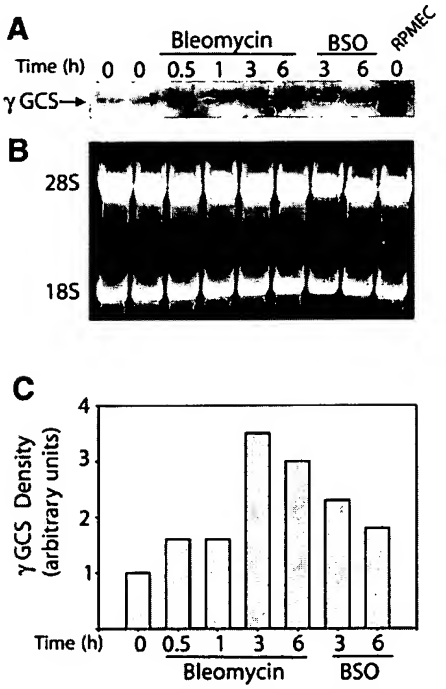

Fig. 2. Bleomycin induces increased expression of γ-glutamylcysteine synthetase (γ-GCS). BPAEC were grown to confluence and treated with bleomycin (1.0 μg/ml) or buthionine sulfoximine (BSO, 100 μM) for the indicated times before RNA was harvested. *A*: Northern blot for γ-GCS. Rat pulmonary microvascular endothelial cell (RPMEC) RNA was used as a positive control for the position of γ-GCS in the bovine samples. *B*: ethidium bromide staining of the agarose gel of bovine and rat RNAs. The positions of 28S and 18S rRNA are indicated. *C*: densitometry of a Northern blot for γ-GCS. Representative data are shown.

Bleomycin activates NF-κB and the ARE-binding transcription factors Nrf-1 and -2. Studies of human γ-GCS_h gene expression have identified two promoter *cis* elements that are believed to primarily regulate its transcription: the κB element and the ARE (6, 16, 17, 37, 44). Increased expression of γ-GCS_h in response to ionizing radiation, which produces physical and chemical damage in addition to inducing the formation of ROS, is dependent on NF-κB activation (16). However, regulation of γ-GCS_h by xenobiotics and ROS-generating compounds is believed to occur through the activation of proteins that bind to the ARE (17, 37, 44). Because bleomycin induces physical damage to cellular proteins and DNA while at the same time producing ROS, we investigated the activation of DNA binding to both κB and ARE.

A time course of bleomycin treatment showed an increase in DNA-binding activity of NF-κB within 1 h as monitored by EMSA (Fig. 3*A*). Densitometric analysis showed that bleomycin induced an approximately fourfold increase in NF-κB activation in 2 h. This increase in NF-κB activity persisted for at least 24 h (data not shown). NF-κB is activated in coordination with the degradation of its inhibitory subunit, IκB. Western blots show that tumor necrosis factor-α induces rapid degradation of IκB-α within 30 min in BPAEC, whereas bleomycin causes a more gradual degradation (Fig. 3*B*). Western blots of NF-κB p65 subunit were performed as a control, showing that levels of the transcription factor are unchanged by bleomycin treatment (Fig. 3*B*). Supershift analysis of the NF-κB band showed that both the p65 and p50 subunits are involved in the complex activated by bleomycin (Fig. 3*C*).

A number of factors are believed to bind ARE and affect downstream transcription; these include the NF-E2-related factors (Nrf) 1 and 2, the Jun protein family (c-Jun, Jun-B, and Jun-D), c-Fos, and the Maf protein family (c-Maf, hMaf, MafG, and MafK) (7, 8, 14, 17, 23, 40, 41, 44). Factor binding to the ARE increases with bleomycin treatment of BPAEC. EMSA experiments detected a >10-fold increase in the binding of factors to a consensus oligo for ARE, which was detected within 30 min of treatment with bleomycin and persisted for at least 24 h (Fig. 4).

We performed supershift analysis to determine which protein(s) was activated in BPAEC by bleomycin. Preincubation of the nuclear extract with an antibodies specific for Nrf-1 and -2 decreases the density of the shifted ^{32}P-labeled ARE band (Fig. 5*A*). Additionally, the Nrf-2 antibody causes the appearance of an ARE-containing band with increased electrophoretic mobility. These data indicate that the original EMSA band contains Nrf-1 and Nrf-2. Our results further suggest that the faster mobility EMSA band, which forms in the presence of the Nrf-2 antibody, contains another protein bound to the ARE. We have labeled this band ARE + X. Importantly, the antibodies directed against Nrf-1 or -2 do not form complexes directly with the ARE in the absence of nuclear extract (Fig. 5*A*, *lanes 2* and *3*).

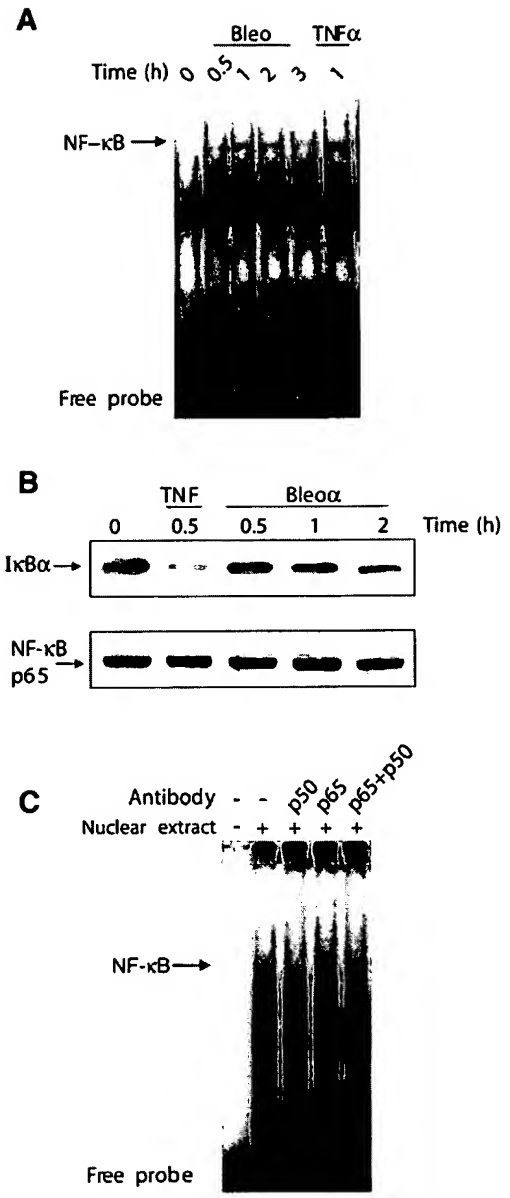

Fig. 3. Bleomycin activates DNA-binding by nuclear factor (NF)-κB and degradation of IκB. *A*: electrophoretic mobility shift assay (EMSA) of protein binding to the κB consensus oligonucleotides. Confluent BPAEC were treated with 1 μg/ml bleomycin (Bleo) or 1 nM tumor necrosis factor (TNF)-α for the indicated times before purification of nuclear extracts. EMSA experiments were performed as described in EXPERIMENTAL METHODS. EMSAs were repeated at least 3 times. The position of NF-κB is indicated. *B*: Western blots of cell lysates after treatment of BPAEC with 1 μg/ml bleomycin or 1 nM TNF-α for the indicated times. *Top*: blotting with antibody directed against IκBα. *Bottom*: same samples blotted using an antibody directed against NF-κB p65 subunit. *C*: supershifts of NF-κB p65 and p50 subunits. Confluent BPAEC were treated with 1 μg/ml bleomycin for 2 h. Nuclear extracts were incubated with 1 μg of antibody against NF-κB p65, NF-κB p50, or both before EMSA was performed. Bleo, bleomycin.

Previous reports have suggested that Nrf-2 may heterodimerize with c-Jun, JunD, MafG, and MafK; these proteins contain DNA-binding domains and are capable of directly binding the ARE (7, 15, 23, 44). An antibody directed against c-Jun did not result in any change in the ARE-containing band, suggesting that c-Jun is not activated by bleomycin and is not involved in Nrf-2 binding to the ARE (Fig. 5*B*). Antibodies directed against c-Fos also caused no change in the ARE binding pattern; this factor is believed to be involved in the inhibition of transcription downstream of ARE (40).

Bleomycin activates ARE-binding via ROS and NF-κB via MAPK. Both ARE and NF-κB site binding factors are known to be activated through a variety of signaling pathways (7, 8, 14, 28, 40, 41, 44, 45). Both the overexpression of the ERK1-MAPK and the induction of ROS activate NF-κB (16, 24, 28). Studies have shown that Nrf-1 and -2 are activated in response to ROS, and the inhibition of ERK1/2-MAPK blocks activation of ARE-binding factors by xenobiotic compounds (17, 40, 44, 45). We previously reported that bleomycin activates the ERK1/2 family of MAPKs (5), and it is widely believed that bleomycin produces ROS through its bound ferrous ion (10, 13, 34, 39). Thus we investigated whether one or both of these mechanisms downstream of bleomycin lead to the activation of factors that bind ARE and/or the NF-κB site.

BPAEC were pretreated for 30 min with *N*-acetylcysteine (NAC), an antioxidant, or U-0126, an inhibitor of MEK1/2 (the kinase upstream of ERK1/2-MAPK). Cells were then treated with ± 1.0 μg/ml of bleomycin for 30 min, and nuclear extracts were prepared. EMSA shows that whereas NAC inhibited bleomycin activation of ARE-binding factors, U-0126 has no effect on the activation (Fig. 6*A*). In contrast, U-0126 blocks bleomycin-induced NF-κB activation, whereas NAC has little or no effect (Fig. 6*B*). Pretreatment of cells with either NAC or U-0126 for 30 min blocks bleomycin upregulation of γ-GCS_h mRNA as determined by Northern blot analysis (Fig. 6*C*).

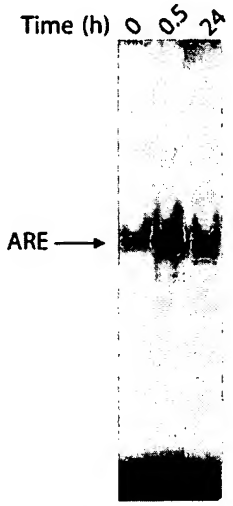

Fig. 4. Bleomycin activates transcription factor binding to the antioxidant response element (ARE) consensus sequence. Confluent BPAEC were treated with 1 μg/ml bleomycin for the indicated times. Nuclear extracts were incubated with the consensus oligonucleotide for ARE. The position of ARE is indicated with an arrow. EMSA experiments were repeated at least 3 times.

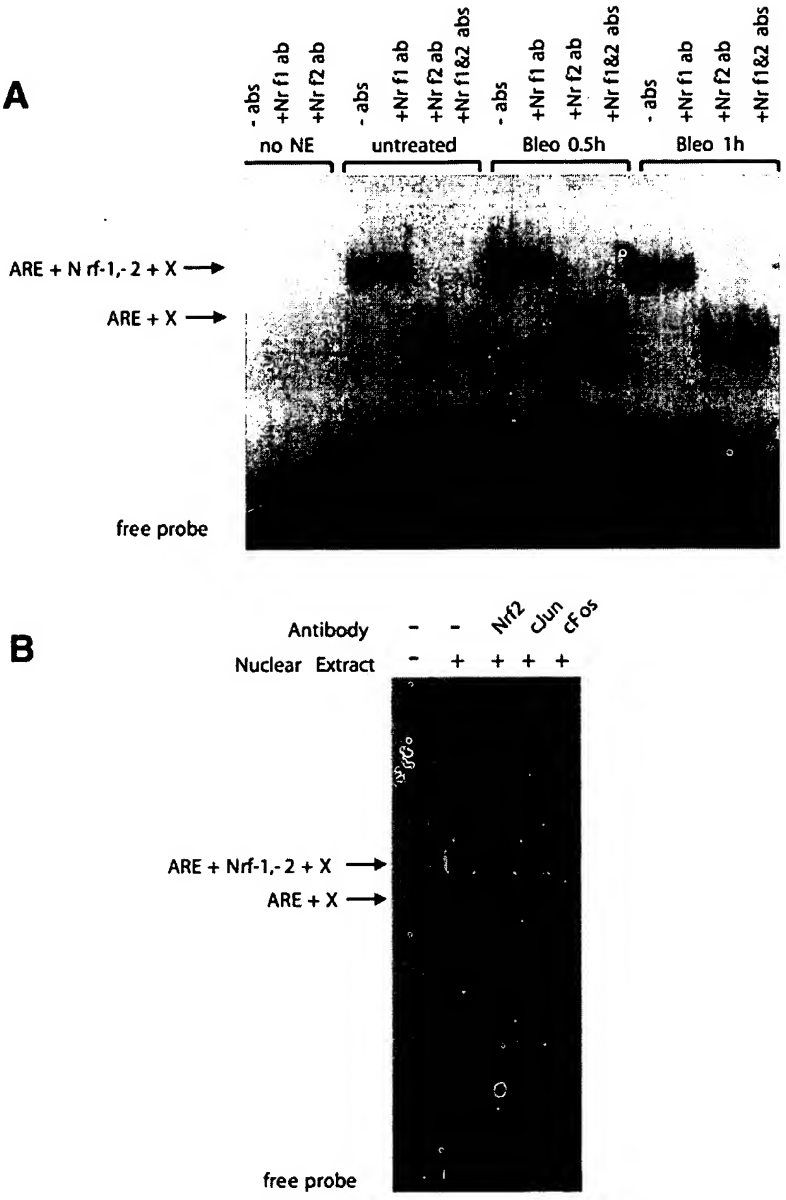

Fig. 5. Bleomycin activates binding of Nrf-1 and -2, but not c-Jun or c-Fos, to the ARE consensus sequence. Confluent BPAEC were treated with 1 μg/ml bleomycin (Bleo) for the indicated times before preparation of nuclear extracts. *A*: EMSAs were performed in the absence and the presence of antibodies (abs) for Nrf-1 and/or Nrf-2 with and without nuclear extract (NE). *Top* arrow: the position of bands containing ARE bound to Nrf-1 and -2 together with an unknown protein(s) X; *bottom* arrow: the position of ARE bound to unknown protein X. *B*: EMSAs were performed in the absence and the presence of antibodies for Nrf-2, c-Jun, or c-Fos. Supershift experiments were repeated at least 3 times.

DISCUSSION

The chemotherapeutic agent bleomycin can induce pulmonary fibrosis, thus limiting its application in cancer treatment in humans. This side effect has been utilized in an animal model system to identify cellular and molecular changes that occur during the development and progression of pulmonary fibrosis (10, 14, 18, 20, 21, 26, 27, 29, 30, 34, 38). Despite extensive work demonstrating the changes in mRNA and protein expression that occur during bleomycin-induced fibrosis, comparatively little is known about the mechanism(s) of these events. The cytotoxic effects of bleomycin are modulated by antioxidants, and we hypothesized that bleomycin regulates cellular defenses against oxidative stress.

The present study indicates that in endothelial cell culture, treatment with sublethal levels of bleomycin (0.01–1.0 μg/ml) for 18 h causes increased total cellular GSH. We also demonstrated that in 30 min, bleomycin increases the level of γ-GCS_h mRNA, the catalytic subunit of γ-GCS that controls the key regulatory step in GSH synthesis. Karam et al. (19) previously reported a ~50% decrease in the level of total GSH in alveolar T2 cells isolated from Wistar rats treated for 7 or 14 days with bleomycin. This was accompanied by a slight decrease in γ-GCS enzyme levels at 7 days. Further experiments are required to determine whether the increase in cellular GSH as observed in the present study would also occur in vivo after acute exposure to bleomycin.

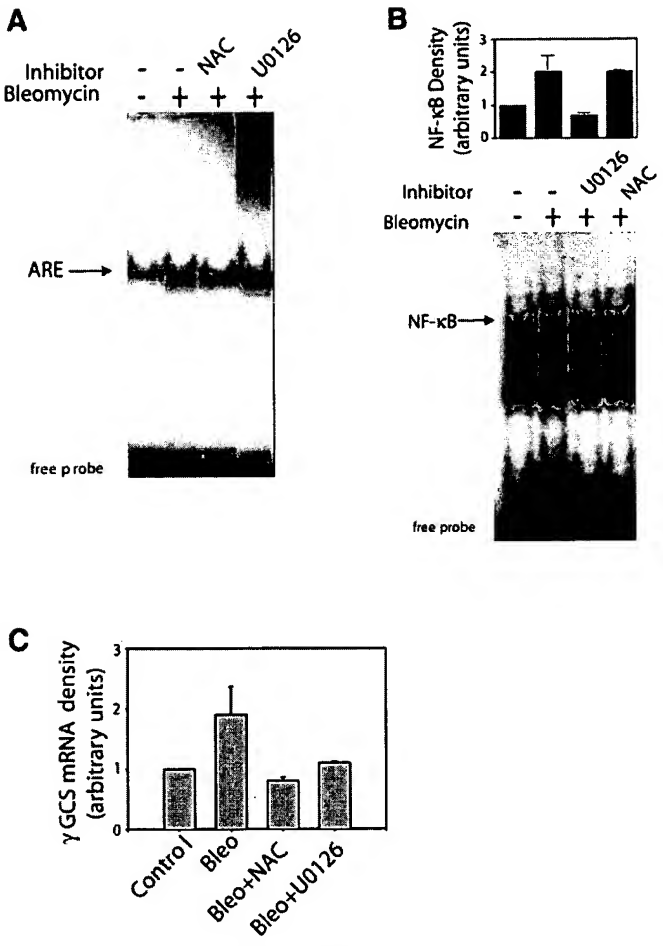

Fig. 6. Bleomycin activation of ARE-binding proteins is dependent upon reactive oxygen species (ROS) generation, but activation of NF-κB is dependent upon extracellular signal-regulated kinase 1/2-mitogen-activated protein kinase (ERK1/2-MAPK). Confluent BPAEC were pretreated with 10 μg/ml U-0126 or 20 mM *N*-acetylcysteine (NAC) for 30 min, then treated with 1 μg/ml bleomycin for 30 min before preparation of nuclear extracts. EMSA experiments were performed as described. *A*: EMSA using ARE consensus oligonucleotide. *B*: EMSA using NF-κB consensus oligonucleotide. Positions of specific bands are indicated. EMSAs with inhibitors were repeated at least 3 times. Densitometry of the NF-κB band is shown above EMSA. *C*: total cellular RNA was extracted, and Northern blot analysis was performed as described for γ-GCS heavy chain (γ-GCS_h). Densitometric quantitation of γ-GCS_h mRNA was performed, and control levels were normalized between experiments. Data show the mean value (n = 3, ±SE).

In response to oxidative or toxic stress, expression of the human γ-GCS_h is positively regulated at the level of transcription by factors binding to both ARE and NF-κB promoter elements (16, 17, 40, 41, 44). Our EMSA results indicate that bleomycin activates both ARE-binding factors and NF-κB in BPAEC within 30 min. Although the sequence of the bovine γ-GCS_h promoter has not been reported, Shi et al. (32, 33) found that endogenous bovine γGCS_h mRNA is increased in BPAEC in response to quinone-induced oxidative stress, similar to findings in other species, including human (44). Therefore, in BPAEC, the induced increase of γ-GCS_h mRNA by bleomycin is consistent with a mechanism involving the induction of ARE-binding factors and NF-κB.

A number of proteins have been shown to bind the ARE element, including Nrf-1 and -2 (members of the cap 'n' collar subfamily of basic region-leucine zipper transcription factors), members of the Jun family (c-Jun, JunB, and JunD), and several small Maf family proteins (c-Maf, hMaf, MafG, and MafK) (7, 8, 14, 17, 23, 40, 41, 44). Supershift experiments using antibodies directed against Nrf-1 or Nrf-2 caused a reduction in the level of the ARE-containing band. However, neither the Nrf-1 nor -2 antibodies caused the appearance of a supershifted species, suggesting that these antibodies dissociate Nrf proteins from a complex with ARE. Inclusion of the antibody against Nrf-2 caused both the reduction of the original ARE-containing band and the appearance of a band with increased electrophoretic mobility. The induction of a band with faster mobility suggests that complexes with Nrf-2 contain at least one additional protein (X) and that the new, faster complex contains the ARE probe bound to X. The identity of X is currently unknown. Other laboratories have shown that Nrf-2 forms heterodimers with small Maf proteins, including MafG (7, 23, 44, 45) and Jun proteins (44). Supershift experiments were performed using antibodies against c-Jun and c-Fos, but these antibodies did not alter the mobility of the ARE complex, indicating that these proteins are not activated by bleomycin.

Nrf proteins have been shown to be activated downstream of protein kinase C and the MAPKs ERK1/2 and stress-activated protein kinase/c-Jun NH_2-terminal kinase (SAPK/JNK) (14, 44, 45). In BPAEC, bleomycin activates p38/HOG1 (unpublished results) and ERK1/2 (5), but not SAPK/JNK (unpublished results). Our current data suggest that bleomycin activates Nrf-1 and -2 through a mechanism independent of ERK1/2-MAPK, as the MEK inhibitor U-0126 failed to block bleomycin induction. Our data showing the inhibition Nrf activation by NAC suggest that ROS act as second messengers downstream of bleomycin.

In contrast to Nrf-1 and -2 activation by bleomycin, NF-κB activation is blocked by U-0126 but not by the ROS-quenching agent NAC, suggesting that the ERK1/2-MAPK pathway is involved. NF-κB activation has been shown to occur in response to the overexpression of ERK1-MAPK (9, 28).

In summary, our results indicate that bleomycin upregulates GSH and γ-GCS through the activation of both ROS- and MAPK-dependent pathways in a mechanism that likely involves the induction of ARE-binding factors and NF-κB. The use of bleomycin in animals remains the most useful model system for the study of pulmonary fibrosis, and the understanding of mechanisms of bleomycin signal transduction pathways should help in developing therapeutic strategies.

We thank Drs. Amy Simon and Daniel Rotiz for technical help.

This work was supported by National Heart, Lung, and Blood Institute Grant HL-42376 and the United States Department of Agriculture (58-1950-9-001). R. Day is a recipient of an American Heart Association National Center Scientist Development Award and an American Lung Association Research Grant.

REFERENCES

1. **Akerboom TPM and Sies H.** Assay of glutathione, glutathione disulfide and glutathione mixed disulfides in biological samples. *Methods Enzymol* 77: 373–382, 1981.
2. **Borzone G, Moreno R, Urrea R, Meneses M, Oyarzun M, and Lisboa C.** Bleomycin-induced chronic lung damage does not resemble human idiopathic pulmonary fibrosis. *Am J Respir Crit Care Med* 163: 1648–1653, 2001.
3. **Cote CG, Yu FS, Zulueta JJ, Vostka RJ, and Hassoun PM.** Regulation of intracellular xanthine oxidase by endothelial-derived nitric oxide. *Am J Physiol Lung Cell Mol Physiol* 271: L869–L874, 1996.
4. **Dasarathy Y, Lanzillo JJ, and Fanburg BL.** Stimulation of bovine pulmonary artery endothelial cell ACE by dexamethasone: involvement of steroid receptors. *Am J Physiol Lung Cell Mol Physiol* 263: L645–L649, 1992.
5. **Day RM, Yongzhen Y, Suzuki YJ, Stevens J, Pathi R, Perlmutter A, Fanburg BL, and Lanzillo JJ.** Bleomycin upregulates gene expression of angiotensin converting enzyme via MAP kinase and Egr-1 transcription factor. *Am J Respir Cell Mol Biol* 25: 613–619, 2001.
6. **Deneke SM and Fanburg BL.** Regulation of cellular glutathione. *Am J Physiol Lung Cell Mol Physiol* 257: L163–L173, 1989.
7. **Dhakshinamoorthy S and Jaiswal AK.** Small Maf (MafG and MafK) proteins negatively regulate antioxidant response element-mediated expression and antioxidant induction of the NAD(P)H:quinone oxidoreductase1 gene. *J Biol Chem* 275: 40134–40141, 2000.
8. **Favreau LV and Pickett CB.** Transcriptional regulation of the rat NAD(P)H:quinone reductase gene. *J Biol Chem* 268: 19875–19881, 1993.
9. **Finkel T.** Oxygen radicals and signaling. *Curr Opin Cell Biol* 10: 248–253, 1998.
10. **Galvan L, Huang CH, Prestayko AW, Stout JT, Evans JE, and Crooke ST.** Inhibition of bleomycin-induced DNA breakage by superoxide dismutase. *Cancer Res* 41: 5103–5106, 1981.
11. **Garner MM and Revzin A.** A gel electrophoresis method for quantifying the binding of proteins to specific DNA regions: application to components of the *Escherichia coli* lactose operon regulatory system. *Nucleic Acids Res* 9: 3047–3060, 1981.
12. **Giaccia AJ, Lewis AD, Denko NC, Cholon A, Evans JW, Waldren CA, Stamato TD, and Brown JM.** The hypersensitivity of the Chinese hamster ovary variant BL-10 to bleomycin killing is due to a lack of glutathione *S*-transferase-α activity. *Cancer Res* 51: 4463–4469, 1991.
13. **Hagimoto N, Kuwano K, Nomoto Y, Kunitake R, and Hara N.** Apoptosis and expression of Fas/Fas ligand mRNA in bleomycin-induced pulmonary fibrosis in mice. *Am J Respir Cell Mol Biol* 16: 19–101, 1997.
14. **Huang H-C, Nguyen T, and Pickett CB.** Regulation of the antioxidant response element by protein kinase C-mediated phosphorylation of NF-E2-related factor. *Proc Natl Acad Sci USA* 97: 12475–12480, 2000.
15. **Ishii T, Itoh K, Takahashi S, Sato H, Yanagawa T, Katoh Y, Bannai S, and Yamamoto M.** Transcription factor Nrf2 coordinately regulates a group of oxidative stress-inducible genes in macrophages. *J Biol Chem* 275: 16023–16029, 2000.
16. **Iwanaga M, Mori K, Iida T, Urata Y, Matsuo T, Yasunaga A, Shibata S, and Kondo T.** Nuclear factor kappa B dependent induction of gamma glutamylcysteine synthetase by ionizing radiation in T98G human glioblastoma cells. *Free Radic Biol Med* 24: 1256–1268, 1998.
17. **Jeyapaul J and Jaiswal AK.** Nrf2 and c-Jun regulation of antioxidant response element (ARE)-mediated expression and induction of γ-glutamylcysteine synthetase heavy subunit gene. *Biochem Pharmacol* 59: 1433–1439, 2000.
18. **Kaminski N, Allarc JD, Pittet JF, Zuo F, Griffiths MJD, Morris D, Huang X, Sheppard D, and Heller RA.** Global analysis of gene expression in pulmonary fibrosis reveals distinct programs regulating lung inflammation and fibrosis. *Proc Natl Acad Sci USA* 97: 1778–1783, 2000.
19. **Karam H, Hurbain-Kosmath I, and Housset B.** Antioxidant activity in alveolar epithelial type 2 cells of rats during the development of bleomycin injury. *Cell Biol Toxicol* 14: 13–22, 1998.
20. **King SL, Lichtler AC, Rowe DW, Xie R, Long GL, Absher MP, and Cutroneo KR.** Bleomycin stimulates pro-α1(I) collagen promoter through TFG β response element by intracellular and extracellular signaling. *J Biol Chem* 269: 13156–13161, 1994.
21. **Koslowski R, Knoch K-P, and Wenzel K-W.** Proteinases and proteinase inhibitors during the development of pulmonary fibrosis in rat. *Clin Chim Acta* 271: 45–56, 1998.
22. **Lowry OH, Rosenburg NJ, Farr AL, and Randall RJ.** Protein measurement with Folin phenol reagent. *J Biol Chem* 193: 265–275, 1951.
23. **Marini MG, Chan K, Casula L, Kan YW, Cao A, and Moi P.** HMAP, a small human transcription factor that heterodimerizes specifically with Nrf1 and Nrf2. *J Biol Chem* 272: 16490–16497, 1997.
24. **Meyer M, Schreck R, and Baeuerle PA.** H_2O_2 and antioxidants have opposite effects on activation of NF-κB and AP-1 in intact cells: AP-1 as secondary antioxidant-responsive factor. *EMBO J* 12: 2005–2025, 1993.
25. **Mulcahy RT, Wartman MA, Bailey HH, and Gipp JJ.** Constitutive and b-naphthoflavone-induced expression of the human γ-glutamylcysteine synthetase heavy subunit gene is regulated by a distal antioxidant response element/TRE sequence. *J Biol Chem* 272: 7445–7454, 1997.
26. **Mutasaers SE, Foster ML, Chambers RC, Laurent GJ, and McAnulty RJ.** Increased endothelin-1 and its localization during the development of bleomycin-induced pulmonary fibrosis in rats. *Am J Respir Cell Mol Biol* 18: 611–619, 1998.
27. **Ortiz LA, Lasky J, Hamilton RF Jr, Holian A, Hoyle GW, Banks W, Peschon JJ, Brody AR, Lungarella G, and Friedman M.** Expression of TNF and the necessity of TNF receptors in bleomycin-induced lung injury in mice. *Exp Lung Res* 24: 721–743, 1998.
28. **Park J-H and Levitt L.** Overexpression of mitogen-activated protein kinase (ERK1) enhances T-Cell cytokine gene expression: role of AP1-NF-AT, and NF-KB. *Blood* 82: 2470–2477, 1993.
29. **Phan SH, Garaee-Kermani M, Wolber F, and Ryan US.** Stimulation of rat endothelial cell transforming growth factor-β production by bleomycin. *J Clin Invest* 87: 148–154, 1991.
30. **Phan SH and Kunkel SL.** Lung cytokine production in bleomycin-induce pulmonary fibrosis. *Exp Lung Res* 18: 29–43, 1992.
31. **Rosso A, Mitchell JB, McPherson S, and Friedman N.** Alteration of bleomycin cytotoxicity by glutathione depletion or elevation. *Int J Radiat Oncol Biol Phys* 10: 1675–1678, 1984.
32. **Shi MM, Iwamoto T, and Forman HJ.** γ-Glutamylcysteine synthetase and GSH increase in quinone-induced oxidative stress in BPAEC. *Am J Physiol Lung Cell Mol Physiol* 267: L414–L421, 1994.
33. **Shi MM, Kugelman A, Iwamoto T, Tian L, and Forman HJ.** Quinone-induced oxidative stress elevates glutathione and induces γ-glutamylcysteine synthetase activity in rat lung epithelial L2 cells. *J Biol Chem* 269: 26512–26517, 1994.
34. **Sikic BI.** Biochemical and cellular determinants of bleomycin cytotoxicity. *Cancer Surv* 5: 81–91, 1986.
35. **Suzuki YJ, Forman HJ, and Sevanian A.** Oxidants as stimulators of signal transduction. *Free Radic Biol Med* 22: 269–285, 1997.
36. **Tian L, Shi MM, and Forman HJ.** Increased transcription of the regulatory subunit of γ-glutamylcysteine synthetase in rat lung epithelial L2 cells exposed to oxidative stress or glutathione depletion. *Arch Biochem Biophys* 342: 126–133, 1997.
37. **Tsan M-F, Danis EH, del Vecchio PJ, and Rosano CL.** Enhancement of intracellular glutathione protects endothelial

cells against oxidant damage. *Biochem Biophys Res Commun* 127: 270–276, 1985.
38. **Vaccaro CA, Brody JS, and Snider GL.** Alveolar wall basement membranes in bleomycin-induced pulmonary fibrosis. *Am Rev Respir Dis* 132: 905–912, 1985.
39. **Venkatesan N, Punithavathi V, and Chandrakasan G.** Curcumin protects bleomycin-induced lung injury in rats. *Life Sci* 61: PL51–PL58, 1997.
40. **Venugopal R and Jaiswal AK.** Nrf1 and Nrf2 positively and c-Fos and Fra1 negatively regulate the human antioxidant response element-mediated expression of NAD(P)H:quinone oxidoreductase1 gene. *Proc Natl Acad Sci USA* 93: 14960–14965, 1996.
41. **Venugopal R and Jaiswal AK.** Nrf2 and Nrf1 in association with Jun proteins regulate antioxidant response element-mediated expression and coordinated induction of genes encoding detoxifying enzymes. *Oncogene* 17: 3145–3156, 1998.
42. **Wang B and Williamson G.** Detection of a nuclear protein which binds specifically to the antioxidant responsive element (ARE) of the human NAD(P)H:quinone oxidoreductase gene. *Biochim Biophys Acta* 1219: 645–652, 1994.
43. **White AC, Das SK, and Fanburg BL.** Reduction of glutathione is associated with growth restriction and enlargement of bovine pulmonary artery endothelial cells produced by transforming growth factor-β_1. *Am J Respir Cell Mol Biol* 6: 364–368, 1992.
44. **Wild AC and Mulcahy RT.** Regulation of the γ-glutamylcysteine synthetase subunit gene expression: insights into transcriptional control of antioxidant defenses. *Free Radic Res* 32: 281–301, 2000.
45. **Yu R, Lei W, Mandlekar S, Weber MJ, Der CJ, Wu J, and Kong A-NT.** Role of a mitogen-activated protein kinase pathway in the induction of phase II detoxifying enzymes by chemicals. *J Biol Chem* 274: 27545–27552, 1999.
46. **Zhang H-Y, Gharaee-Kermani M, Zhang K, Kaminol S, and Phan SH.** Lung fibroblast α-smooth muscle actin expression and contractile phenotype in bleomycin-induced pulmonary fibrosis. *Am J Pathol* 148: 527–537, 1996.

This Page is Inserted by IFW Indexing and Scanning Operations and is not part of the Official Record

BEST AVAILABLE IMAGES

Defective images within this document are accurate representations of the original documents submitted by the applicant.

Defects in the images include but are not limited to the items checked:

- ☐ BLACK BORDERS
- ☐ IMAGE CUT OFF AT TOP, BOTTOM OR SIDES
- ☐ FADED TEXT OR DRAWING
- ☐ BLURRED OR ILLEGIBLE TEXT OR DRAWING
- ☐ SKEWED/SLANTED IMAGES
- ☑ COLOR OR BLACK AND WHITE PHOTOGRAPHS
- ☐ GRAY SCALE DOCUMENTS
- ☐ LINES OR MARKS ON ORIGINAL DOCUMENT
- ☐ REFERENCE(S) OR EXHIBIT(S) SUBMITTED ARE POOR QUALITY
- ☐ OTHER: _____

IMAGES ARE BEST AVAILABLE COPY.
As rescanning these documents will not correct the image problems checked, please do not report these problems to the IFW Image Problem Mailbox.